Title

Biomaterial-Mediated Immunomodulation Via The Implantation of Drug-Eluting Vascular Grafts

Author

Vu, Tan Phat

Publication Date

2023

Peer reviewed|Thesis/dissertation

UNIVERSITY OF CALIFORNIA

Los Angeles

Biomaterial-Mediated Immunomodulation Via The Implantation of Drug-Eluting Vascular Grafts

A thesis submitted in partial satisfaction of

the requirements for the degree of Master of Science

in Bioengineering

by

Tan Phat Vu

2023

ABSTRACT OF THE THESIS

Biomaterial-Mediated Immunomodulation Via

The Implantation of Drug-Eluting Vascular Grafts

by

Tan Phat Vu

Master of Science in Bioengineering

University of California, Los Angeles, 2023

Professor Song Li, Chair

Graft rejection is an immunological response facilitated by the host T lymphocytes and this process could engender tissue destruction and alloantibody production. Allograft recipients must adhere to a rigorous immunosuppressant administration to avoid post-operative complications to the graft. Herein, an acellular drug-eluting vascular graft platform was proposed to alleviate the requirement for systemic drug administration via the targeted delivery of tacrolimus. The graft inner layer and drug-carrying matrix were electrospun with poly(L-lactide-co-caprolactone)/poly(D,L-lactic-co-glycolic acid) as the inner layer and poly(carbonate-urethane) as the outer layer. Mechanical characterization and degradation kinetics of the engineered graft were performed and the optimal material composition was determined. In vitro cytocompatibility assays utilizing endothelial cells, macrophages, and T-cells of primary sources were done and the optimal

drug loading concentration was identified. The anastomosis of the drug-eluting vascular graft into the femoral artery of rats was performed to assess its in vivo tissue integration and therapeutic capability. This experimental approach was devised as a proof-of-concept study prior to an elaborate organ transplantation model. The graft maintained a high patency rate and a sustained concentration of tacrolimus after a month of implantation, therefore proving the feasibility of a novel biomaterial-mediated immunomodulation modality.

The thesis of Tan Phat Vu is approved.

Jun Chen

Timothy J. Deming

Song Li, Committee Chair

University of California, Los Angeles

2023

Table of Contents

Table of Figures

Acknowledgments

Firstly, I would like to express my gratitude towards the department chair and my research advisor, Dr. Song Li, for his considerate and comprehensive guidance throughout my time in research. Professor Song Li, despite his hectic schedule, managed to provide constructive feedback for my research and acknowledged my contribution to his laboratory. I was blessed with the opportunity to work under his scientific direction.

Secondly, I would like to thank Dr. Zeyang Liu for his inspiration and observations during the creation of my master's research project. Dr. Liu was always present in the laboratory for the continuous support and insightful troubleshooting of the experiments.

Thirdly, I would like to extend my appreciation to Dr. Jun Chen and Dr. Timothy J. Deming for serving on my master's thesis committee. The revision of my thesis was made possible through your precious time and effort.

Fourthly, and most profoundly, I would like to thank the members and collaborators of Dr. Song Li's laboratory, namely Jennifer Soto for the routine management; Xinyang Ge for her collaborative assistance during experimental protocols; Yu Zhu for his instructional endeavors during cell culture and characterization experiments; Youcheng Yang for his exceptional data presentation and scanning electron microscopy experiments; Xiao Han for the quantitative polymerase chain reaction and enzyme-linked immunosorbent assay experiments; Dr. Tzuchun Chung, Dr. Hidenobu Kojima, and Dr. Abbas Ardehali for the animal implantation surgeries; and Tyler Hoffman for the Doppler ultrasonography experiments. This journey was a life-altering experience and I have learned so much from everyone in the Department of Bioengineering and the Division of Laboratory Animal Medicine.

Finally, my acknowledgment could not be without the Vingroup Science and Technology Scholarship Program for Overseas Study of Higher Education for their financial support of the degree.

To my parents, Võ Thị Thanh Thảo and Vũ Ngọc Hiển,

My academic prowess was cultivated through your unconditional love and resolute determination. The pursuit of this master's degree was founded on your continual encouragement and rapport since the start of my education path. Thank you for everything.

Chapter 1 Introduction to Tissue-Engineered Vascular Grafts

1.1 Anatomy and Physiology of Blood Vessels

The circulatory system, particularly blood vessels, is physiologically integral to the human body. Blood vessels transport oxygen, glucose, amino acids, hormones, and growth factors to healthy tissues, while simultaneously discarding carbon dioxide and metabolic byproducts. Except for capillaries, all blood vessels are composed of three main cellular layers: the tunica intima, tunica media, and tunica adventitia (Figure 1) [1].

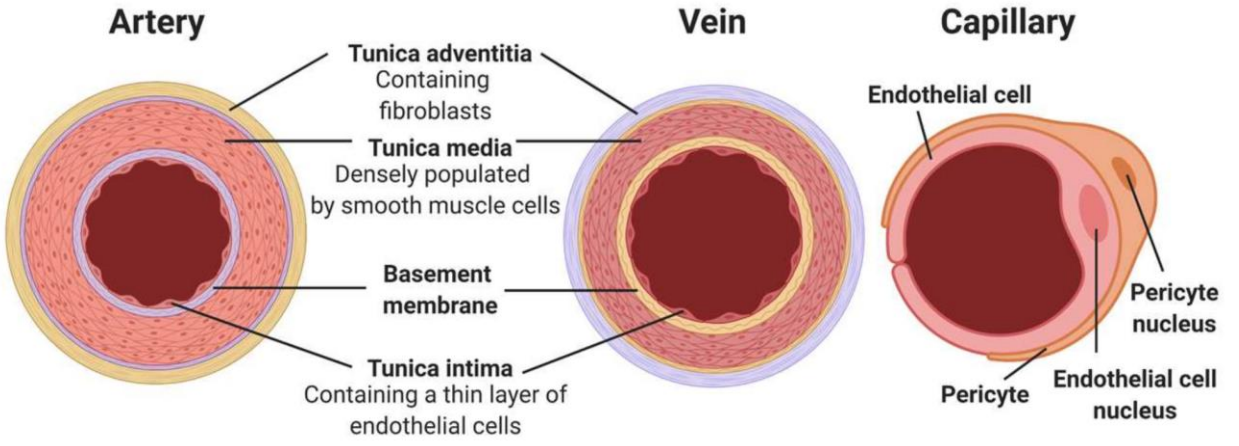

Figure 1. Anatomical Features of the Blood Vessel [1]

For each layer of the artery and the vein, there exists a primary cell type; namely endothelial cells for the intimal layer, vascular smooth muscle cells for the medial layer, and fibroblasts for the adventitial layer. The endothelial cells (EC) line a single layer inside all blood vessels that modulate physical and chemical cues between the bloodstream and neighboring tissues. For instance, an abnormality in the endothelial lining could activate the coagulation cascade and local inflammation at the injured site. EC also facilitates a smooth surface for the laminar flow of blood and selective diffusion for bioactive molecule transport. The smooth muscle cells (SMC) maintain

vascular homeostasis through active contraction and relaxation. In diseases such as hypertension and atherosclerosis, this function is inhibited concurrently with the changes in the mechanical environment surrounding vascular smooth muscle cells [2]. Vascular SMC is the main regulator of blood pressure through calcium-dependent contraction. Interspersed among the SMC layers is a comprehensive array of extracellular matrix (ECM) containing elastin and collagen fibers. The function of collagen is to provide mechanical support for the arteries, while that of elastin is to supplement elasticity for vessel distensibility. Lastly, the adventitia consists of lymphatic vessels, nerve fibers, and connective tissues. As fibroblasts are the principal cellular makeup of the adventitia, they orchestrate a distinct response to injury, hypoxia, and pulmonary hypertension and mediate vascular remodeling, repair, and extracellular matrix deposition [3]. The ECM composition of these three layers is not similar from arteries to veins since the requirements for conduit openings, blood transport, and vessel compliance might differ. For instance, the proteins prevalently expressed in the extracellular matrix elastic arteries (5 - 30 mm) are elastin, fibronectin, fibrillin, fibulin, collagen (type I, II, III, IV, V, and VI), and proteoglycans [4].

1.2 Design Requirements for Bioengineered Vascular Grafts

In 1954, Dr. DeBakey and his colleagues implanted the first prosthetic graft made of polyethylene terephthalate into a patient for the augmentation of the weakened arteries. Ever since this revolutionary invention, bioengineers, clinical scientists, and medical practitioners have attained stupendous advances in the creation of vascular conduits in healthcare. A bioengineered vascular graft should display the following attributes [1, 5–8]: being biologically compatible (exhibiting non-immunogenicity, sustaining patency, withstanding degradation, supporting vascularization, mitigating thrombogenesis, and promoting regeneration) and being mechanically

compatible (retaining suturability, precluding leakage, possessing compliance, and showcasing durability).

As mentioned, the engineered graft needs to be non-cytotoxic to the neighboring cells and non-immunogenic to the constituents of the immune system (e.g., complement proteins, resident macrophages, circulating neutrophils, or other adaptive immunity effectors). The graft also needs to maintain patent throughout its in situ integration with the native vessels. Moreover, recent endeavors in designing a tissue-engineered vascular graft (TEVG) have focused on the ability of a graft to be safely metabolized by the body, i.e., biodegradability. This is of inspiring essence as it allows for pharmacological agents or growth factors to be embedded in the polymeric matrix, therefore releasing the desired molecule in a precise spatial and temporal setting after a hydrolysis reaction. As depicted in [6], transplantable grafts can be designed to accelerate vascular integration and graft perfusion, which leads to the prevention of thrombotic events. Revascularization is critical to the implantation of vascular grafts since coagulation factors such as the Willebrand factor and tissue factor will accumulate as soon as an immature vasculature network is presented on engineered constructs. Vascular graft failures are most commonly associated with unintended thrombosis [7]. The luminal surface of the graft should simultaneously be taken into account, as geometric and hemodynamic effects of the surface might trigger thrombogenesis. The TEVG luminal surface must avoid negative inflammatory responses (e.g., protein deposition, platelet activation, or leukocyte adhesion) and thrombogenesis immediately upon implantation and promote endothelialization [8]. Finally, the TEVG should serve its main purpose: as a platform for cellular proliferation, structural remodeling, and functional recapitulation in vivo. This objective could be accomplished via an array of biofabrication processes, chemical modifications, and physical alterations.

Additionally, the bioengineered graft, while in the design phase, must be ascertained of structural integrity, such as the ability to withstand hemodynamic pressure or aneurysmal deformation. It is expected that the replacement graft will be sutured to an area of weakened vessels. Thus, the burst strength and mechanical modulus of the graft must be designed such that the TEVG can withstand physiological conditions. The graft should possess suitable compliance to prevent the formation of high stresses around the anastomosis and be of a geometry that does not induce certain, undesirable, flow characteristics as both of these factors have been associated with failures in current bypass solutions [7].

Aside from the engineering standpoints, the TEVG must prove befitting clinical standards, such as the ability to be handled, manipulated, and sutured; and be able to be mass produced in a range of lengths, quality controlled, stored, and shipped at an economically viable cost [7].

1.3 Engineered Scaffolds for Vascular Tissue Engineering

With certainty, autologous vascular tissues will always be the gold standard for cardiovascular reconstitution since they can attenuate immunological complexity and structural mismatch. Nevertheless, autologous grafts are of limited availability or adequacy. Moreover, their harvest adds time, cost, and the potential for additional morbidity to the surgical procedure [9]. To overcome the limitations associated with autologous and synthetic graft transplantation, the concept of tissue engineering was proposed [10]. Tissue engineering is a scientific field that may solve the problems that plague current grafts. Tissue engineering is defined as an interdisciplinary field that combines engineering and biomedical principles to create materials that integrate with a patient's native tissue to restore or improve physiological function [11]. The classical paradigm of tissue engineering includes:

(I) Cells (i.e., progenitor cells, stem cells);

(II) Scaffolds (i.e., synthetic, decellularized extracellular matrix);

(III) Signals (growth factors, chemotactic factors) [10, 11].

Implantable three-dimensional (3D) scaffolds are used for the restoration and reconstruction of different anatomical defects of complex organs and functional tissues. The scaffolds provide a template for the reconstruction of defects while promoting cell attachment, proliferation, extracellular matrix generation, and restoration of vessels, nerves, muscles, bones, etc. Scaffolds are 3D porous, fibrous, or permeable biomaterials intended to permit fluid transport, promote cell interaction, maintain cell viability, and ensure ECM deposition with the minimum inflammation and toxicity while bio-degrading at a controlled rate [12]. The implementation of biomaterial-based scaffolding constructs offers a myriad of advantages. Firstly, scaffolds obviate the need for drug administration or cell therapy and therefore a tunable approach that has been used for decades to suit the physician's requirements and the patient's needs. A scaffold, owing to its mechanical or chemical cues, can direct cellular behavior and induce favorable reactions (e.g., angiogenesis and vasculogenesis). Secondly, scaffolds can be engineered to be a delivery platform for drugs, biomacromolecules, or cells, as they release the active components at a desired release rate with definitive spatial control and enable drug protection before bodily contact [13]. Over the past years, the paradigm shift in scientific research has been placed on scaffolds for tissue engineering and drug delivery. A quick search on the Scopus database as of March 2023 returned 95,050 papers with the combinatory keywords of "scaffolds", "tissue engineering", and "drug delivery" [14]. Figure 2 was generated through the VOSviewer software [14], displaying the multifarious applications and innovations of biomedical scaffold engineering in the first quarter of 2023.

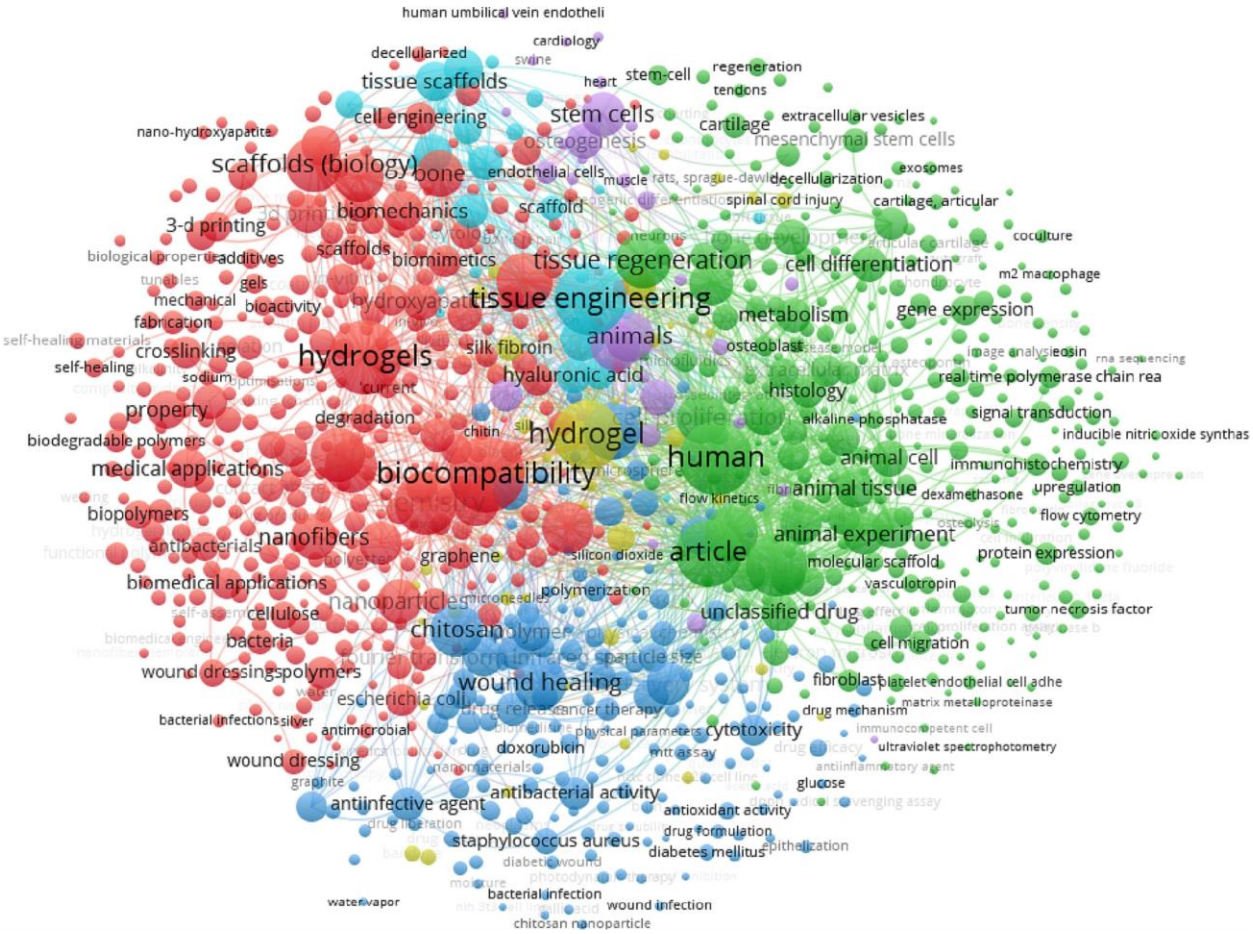

Figure 2. Bibliometric map of published works in 2023, obtained using VOSviewer software version 1.6.16, using “Scaffolds” AND “Tissue Engineering” AND “Drug Delivery” as combined keywords, recorded from the Scopus database (March 22nd, 2023), limited to the first 2000 publications and screening the abstract, author and index keywords [14].

Prosthetic vascular grafts or tissue-engineered vascular grafts were of clinical prominence because of the reproducibility and tunability of synthetic, bioinspired, or biohybrid materials. The impending sections will outline the biomaterials apropos to the development and utilization of engineered scaffolds for vascular tissue engineering.

1.3.1 Synthetic Polymers

Synthetic materials have been employed in vascular graft design for a variety of reasons, mainly due to the ease and flexibility of tailoring their mechanical properties [9]. In the case of poor autologous graft harvest or quality, prosthetic vascular grafts will be employed to salvage the deteriorating functions, be it for surgical revascularization [15] or hemodialysis access [16]. These clinical applications were based on the ability of a synthetic material to exact patient specificity, in geometrical size and physiological distinctiveness. The tunability of synthetic materials has proven beneficial for drug delivery and tissue engineering applications, and the functionalization or coating of the materials can be done to reduce acute thrombogenesis, increase antimicrobial resistance, or prolong luminal patency. For instance, heparin functionalization could bolster the performance of TEVGs in vivo, as the enhancement in hydrophilicity and water absorption of the surface-functionalized nanostructures favored the adhesion and proliferation of human adipose-derived stem cells [17]. In addition, multiple TEVGs have been approved by the Food and Drug Administration (FDA) for clinical and therapeutic usage. Synthetic grafts, nonetheless, are also capable of initiating an inflammatory response, due to their pH-lowering degradation effects [18, 19] or lacking peptide domains for cell adhesion and proliferation [20, 21].

1.3.1.1 Bioinert Polymers

"Bioinert" (or nondegradable) polymers, such as expanded polytetrafluoroethylene (ePTFE), polyethylene terephthalate (trade name: Dacron®), and polyurethane have been widely studied and used since the early days of vascular engineering to create vascular substitutes [22, 23].

ePTFE is a porous polymer with an electronegative luminal surface that is not degradable, and the polymer was manufactured via extrusion. However, only 45% of standard ePTFE grafts are patent as femoropopliteal bypass grafts at 5 years, while autologous vein grafts display a 60–80% patency [9, 24, 25]. ePTFE is rarely used for grafts of small diameters (<6 mm), for its innate hydrophobicity that activates the coagulation cascade [20, 26], low permeability that obstructs nutrient diffusion [23, 27], and absence of binding motifs for cell adhesion [28]. ePTFE could still be employed for engineered grafts, with modifications to ensure a more biocompatible interaction with the native tissue. The authors in [26] developed a solution to circumvent ePTFE hydrophobicity by coating the surface of the scaffold with ECM proteins and CD34 monoclonal antibodies. The modified ePTFE decreased the hemolysis and platelet adhesion rate, while significantly increasing the adhesion of endothelial cells on the grafts [26]. The authors in [28] modified ePTFE by grafting the endothelial cell's specific peptide arginine-glutamic acid-aspartic acid-valine (REDV) using bifunctional polyethylene glycol (PEG)-spacer (known to increase hydrophilicity and reduce platelet and nonspecific protein adhesion) and retrieved favorable results. PEG-mediated peptide immobilization was concluded to have rendered PTFE an excellent substrate for cellular growth while simultaneously endowing the material with antifouling properties [28].

Polyethylene terephthalate (PET) grafts are often crimped longitudinally to increase flexibility, elasticity, and kink resistance. However, these properties are lost soon after implantation, as a consequence of tissue ingrowth [9]. It was reported that platelet deposition and complement activation are lower on ePTFE than on PET grafts [29–31]. As stated by a meta-analysis study on 91 publications [32], primary patency was similar between ePTFE and PET prostheses, secondary patencies were better with PET at 10 years. Notwithstanding antiplatelet

and anticoagulation therapies in these trials, it can be concluded that Dacron prosthetic grafts are superior to PTFE grafts in arterial bypass procedures [32].

Polyurethane is a copolymer that consists of three different monomer types: a diisocyanate hard domain, a chain extender, and a diol soft domain. At physiological temperatures, the soft domains provide flexibility, while the hard domains impart strength. The most common medical-grade polyurethanes are based on soft domains made from polyester, polyether, or polycarbonate [9, 33]. A polyurethane derivative with poly(carbonate) soft segments (PCU) was shown to exhibit similar compliance properties to human arteries post-implantation [33]. It was stated that the compliance of the PCU graft did not change after the perivascular penetration and remodeling in vivo, which was a rather common reaction for other conventional prosthetic grafts. In a clinical study on 17 humans in 2011 [34], electrospun PCU grafts were implanted in patients for early hemodialysis access. Not only did the grafts not evoke any systemic or local complications, but post-implantation vascular access needs were also met entirely by the graft in every instance. PCU grafts also prevented the need for venous catheters. The electrospun polycarbonate-urethane graft was thus considered safe in humans, with the equivalent patency continuing up to 12 months [34]. PCU can also be synthesized with degradable moieties, which can promote rapid complete endothelialization, increased transmural cellular ingrowth, sustained proliferation of cells, and non-inflammatory microvessel formation [35].

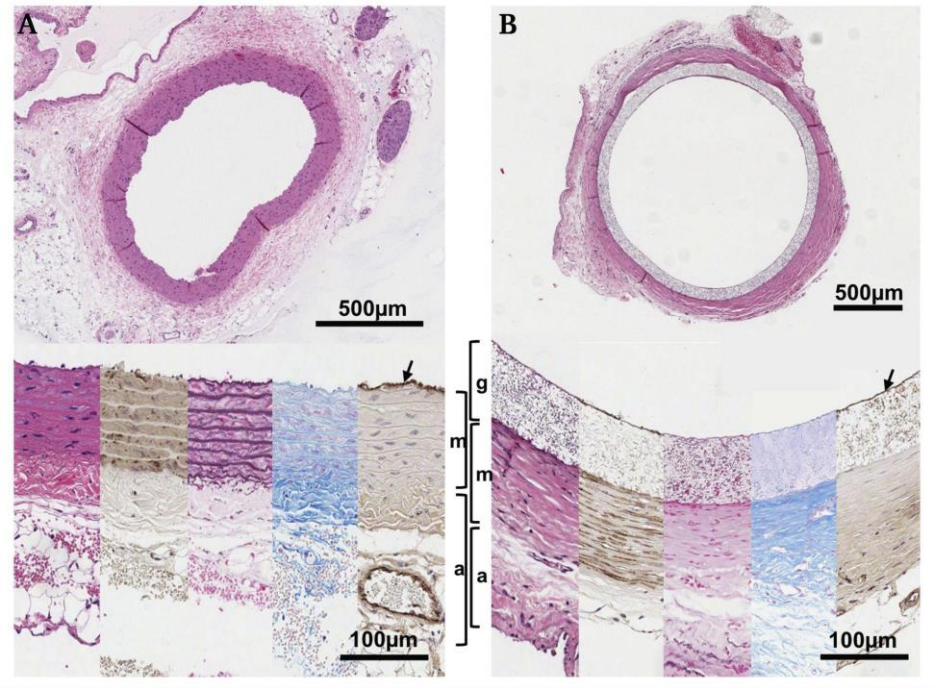

Figure 3. Architecture of the integrated degradable polycarbonate urethane (dPCU) graft in direct comparison to the native abdominal aorta. The natural vessel's structure (A) consists of the intima (arrow), media (m), and adventitia (a). After implantation of the dPCU graft, the architecture was soon restored and the layers were discernible (B). The graft was incorporated between neointima and neomedia (12 months of implantation, n = 7). Stainings from left to right: hematoxylin eosin, smooth muscle actin, elastica, anilin blue, von Willebrand factor [35].

The in vivo implantation of degradable PCU grafts into rodents was proven successful, as Figure 3 depicts the sustained patency of these grafts, without the signs of plaque, thrombus, or calcification.

1.3.1.2 Biodegradable Polymers

Biodegradable polymers are considered “biocompatible” since they can be safely metabolized during biochemical cycles of the human body. Bioengineers could exploit this concept

to design a polymeric reservoir “loaded” with bioactive compounds, and concurrent with the degradation of the bulk matrix, these biofactors could be released to the local environment in a controlled manner. A successful scaffold should balance mechanical function with biofactor delivery, providing a sequential transition during which the regenerative signals are accumulated or the inflammatory effectors are negated as the scaffold degrades. This balance often presents a tradeoff between a denser scaffold (providing better function) and a more porous scaffold (providing better biofactor delivery) [36]. The advantage of a biodegradable approach includes continuous remodeling of graft until an endogenous neovessel has formed. Prerequisites for degradable materials are adequate biomechanical stability until tissue formation has occurred to avoid vessel leakage, conduit rupture, and aneurysm formation [37], in conjunction with the several design requirements noted in section 1.2.

The upcoming sections will delineate the most prevalent biodegradable polyesters used in biomedical engineering research and clinical trials, namely poly(D/L-lactic acid) (PLA), poly(glycolic acid) (PGA), poly(ε-caprolactone) (PCL), the copolymer poly(D,L-lactic-co-glycolic acid) (PLGA), and the copolymer poly(L-lactide-co-caprolactone) (PLCL). Some of these polymers have been approved for human usage by the FDA. It should be noted that the list is not exhaustive, as there are other classes of biodegradable polymers such as polyanhydrides, polyamides, polyalcohols, or polyhydroxyalkanoates.

PLA is a hydrophobic (contact angle ~ 80° [38]) and aliphatic polyester. Two types of PLA are used in biomedical research: poly-L-lactic acid (PLLA) and poly-D-lactic acid (PDLA). PLLA has a melting point of 173–178°C (semi-crystalline polymer), glass transition temperature of 60–65°C, modulus of 2.7 GPa, elongation of 5–10%, and degradation time of >24 months [39]. PDLA does not have a melting point (amorphous polymer), glass transition temperature of 55–60°C,

modulus of 1.9 GPa, elongation of 3–10%, and degradation time of >12–16 months [39]. During non-enzymatic hydrolysis in biological tissues, the polymer degrades into monomers of lactic acid, which is a naturally occurring byproduct of biochemical processes [40]. Apart from its biocompatibility, adjustable biodegradability, and suitable mechanical properties, PLA has good processability by additive manufacturing (AM) techniques (ISO/ASTM 52900:2015), allowing for the development of patient-specific constructs [41]. PLA has been approved by the FDA for various clinical products: absorbable sutures, cell carriers, implantable scaffolds, and other biomedical devices. As drug delivery systems, PLA electrospun fibers have been programmed to circumscribe lumen stenosis [42] and tumor progression [43] in recent studies. On the other hand, PLA scaffolds also have been associated with major demerits, such as undesirable inflammation due to acidic changes in the microenvironment pH, unimprovable surface characteristics due to the deficiency of reactive side groups, and the unfavorable biomaterial-tissue interaction due to PLA's inherent hydrophobicity.

PGA is the most widely used biodegradable polymer, for its high flexibility [44], low immunogenicity [45], and sustained graft patency [46]. It is the first biodegradable polymer to be used as sutures [13]. PGA has a melting point of 225–230°C (semi-crystalline polymer), glass transition temperature of 35–40°C, modulus of 7.0 GPa, elongation of 15–20%, and degradation time of 6–12 months [39]. PGA hydrolyzes into glycolic acid monomers. PGA is more hydrophilic than PLA or PCL (contact angle ~ 65° [47]), so it degrades at a more rapid rate. While this characteristic provides an advantage in tissue remodeling, PGA alone degrades too fast and loses its mechanical strength before the remodeled tissue obtains sufficient durability, resulting in graft fracture or aneurysmal formation [20]. PGA loses its strength in vivo within four weeks and is completely absorbed by six months [10]. To repress this unwanted performance of the polymer,

engineers added other polymers such as PCL, PLCL, or PLGA to slow the in vivo degradation rate, introducing satisfactory remodeling observed for up to six months [44, 48, 49]. Its degradation, signified by the hydrolysis of the ester bond, could therefore be regulated with the copolymerization with other (more hydrophobic) polymers. PGA is also authorized by the FDA for clinical and commercial applications.

PCL serves as the most commonly used polymer in vascular scaffolds due to its excellent biocompatibility, suitable in vivo degradation kinetics, low cost, mature fabrication techniques, and off-the-shelf properties [44]. It also has high printability and blend-ability [13], which are useful in bioprinting or biofabrication of structures. PCL has a melting point of 58–63°C (semi-crystalline polymer), glass transition temperature of –65°C, modulus of 0.4 GPa, elongation of 300–500%, and degradation time of >24 months [39]. PCL has a slower degradation rate than PLA and PGA. Its hydrolyzed degradation is based on the bulk erosion of the entire molecular structure. At the latest stages of in vivo degradation, after the fragmentation of the PCL chain into low-molecular-weight fragments, intracellular degradation can take place by phagocytosis [50, 51]. PCL has a contact angle of ~140° [52]. As a vascular graft, PCL underwent structural compliance of 70% and endothelial coverage of 70% at nine months post-implantation into rodents [53].

PLGA is a readily available commercial biodegradable polymer (also FDA-approved), owing to its desirable physicochemical and biocompatible characteristics in vivo [54, 55]. As a copolymer of PLA and PGA, PLGA could be tailored to fit the desired degradation rate by choosing the ratio of lactide and glycolide constituents. At the ratio of lactide:glycolide of 50:50, PLGA has no melting point (amorphous polymer), glass transition temperature of 45–50°C, modulus of 2.0 GPa, elongation of 3–10%, and degradation time of 1–2 months [39]. As the ratio of PLA increases in the random copolymer chain, the degradation rate increases up to 5–6 months

at a lactide:glycolide ratio of 85:15 [39]. The contact angle of PLGA is approximately ~75° [55]. It was demonstrated that a year after the implantation of PLLA/PGA TEVGs, the scaffolds maintained their patency with the regeneration of endothelial cells (representative of the tunica intima), smooth muscle cells (representative of the tunica media), and elastin/collagen fibers (representative of the tunica adventitia) in a canine carotid artery [56] and porcine aortic interposition models [57]. PLGA is implemented in drug delivery systems (e.g., microspheres), surgical sutures, polymeric scaffolds, and plasmonic nanocomposites [58].

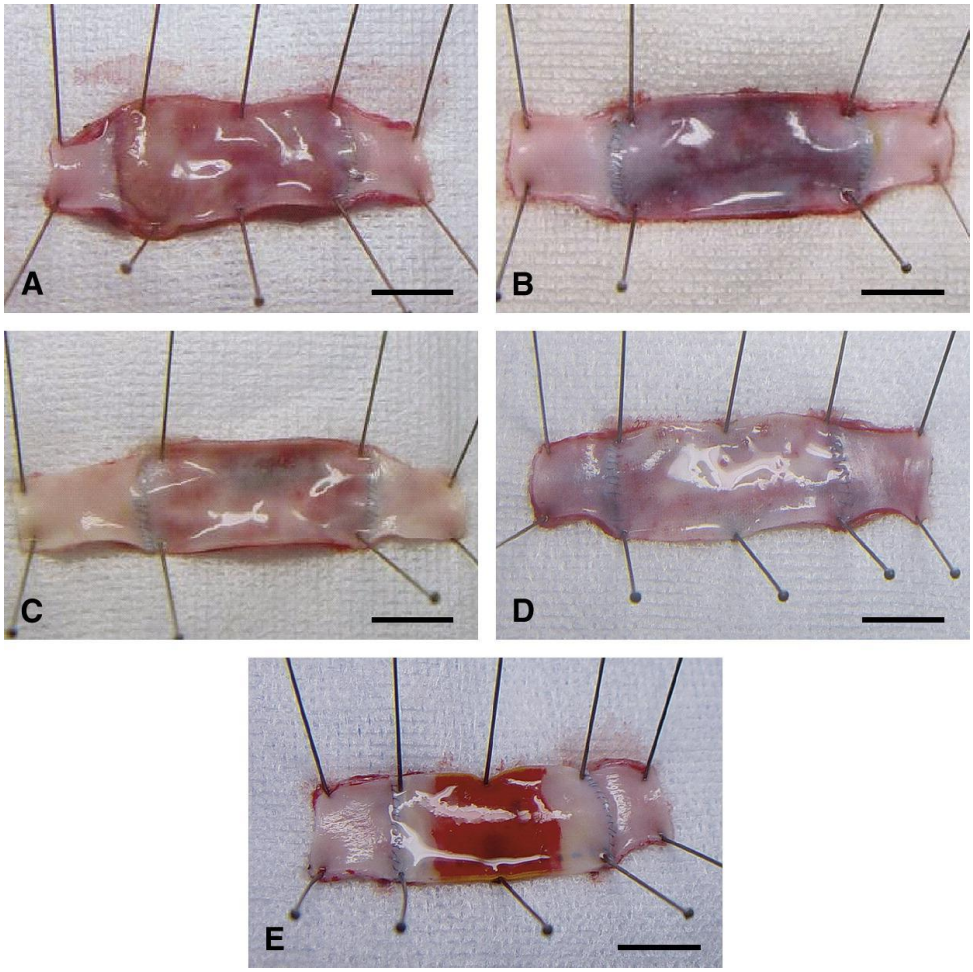

Figure 4. Macroscopic appearance of TEVGs 2 (A), 4 (B), 6 (C), and 12 (D) months after implantation and the ePTFE graft 12 months after implantation (E). The scale bar represents 10 mm. The figure was extracted from [56].

PLCL is a copolymer that can be synthesized via block or random polymerization of L-lactide and ε-caprolactone. The association of PLLA with PCL in the main structure has been reported to compensate for both the brittle behavior of PLA (hard) and the low stiffness of PCL (soft) [59]. Because of this, PLCL is expected to have a modulus between that of PLLA (upper limit) and PCL (lower limit). PLCL has been proven to be suitable for soft tissue engineering materials [59], and more importantly, small-diameter vascular grafts [60–62]. PLCL has low immunogenicity and high endothelization. Per the results reported by [59], PLCL-braided scaffolds witnessed no particular inflammation or degradation four weeks after implantation. The authors of [60] reported an 80% patency rate after ten weeks of implanting electrospun PLCL grafts in rabbits as a carotid artery bypass. It was also depicted that the markers of endothelial cells, smooth muscle cells, and extracellular proteins were discovered in the TEVG at six months, resembling those of the natural compositions of the native artery. Moreover, PLCL has adequate mechano-elasticity properties, resulting in its identification as one of the applicable candidates for vascular tissue engineering.

1.3.2 Natural Polymers

The incorporation of natural biopolymers in vascular scaffolds could provide numerous advantages, attributable to the enhanced biocompatibility, bioactivity, and biomimicry. Natural polymers typically have cell-binding protein motifs that bolster the recruitment, expansion, and colonization of intrinsic cells [63–66]. These polymers also have minimal immunological and

inflammatory responses because they are derived or extracted from the native protein/peptide blocks of the human body (biogenicity). In addition, the degradation products of the hydrolysis or proteolysis reactions are biologically tolerant. Biofunctional groups such as amide, carboxylic acid, sulfide, and alcohol are amenable to chemical conjugations and conversions. Howbeit, natural (bio)polymers have weak mechanical properties, unpredictable degradation rates, inconsistent batch-to-batch homogeneity, and undefined/abstruse biological interactions. Because of these drawbacks, natural polymers are often employed as hybrid TEVGs with the addition of synthetic polymers. The following paragraphs will introduce the most prominent natural polymers in each class, namely collagen and elastin for polypeptides and chitosan and alginate for polysaccharides. It should be noted that there are other classes of natural polymers used in biomedical applications, such as polynucleotides and proteoglycans.

Collagen is the most used natural polymer in vascular tissue engineering [21, 44]. Collagen chemical structure consists of ~33% glycine, ~25% proline or hydroxyproline, ~25% lysine or hydroxylysine, and the balance is other amino acids. Collagen can exist in fibrillar or non-fibrillar forms and is highly conserved in animals. Collagen supports cell adhesion through cell-binding domains. Although it has the advantage of weak antigenicity and robust biocompatibility in vivo [66], collagen as a biomaterial is often discouraged for its inadequate mechanical strength. Consequently, it is usually accompanied by other synthetic polymers in biomedical applications [66–69]. In [69], the researchers developed an electrospun PLA/collagen vascular graft and examined its performance in vitro. The dynamic compliance recorded was similar to that of the human saphenous vein. Furthermore, with the contribution of collagen in the scaffold, the adhesion and proliferation of primary human umbilical vein endothelial cells (HUVEC) also increased. The

elevated concentration of collagen leads to improved hemocompatibility and vascularization, which can be rendered a tradeoff for reduced elasticity and rapid degradation in vivo [68].

Elastin is an elastic and hydrophilic protein that is detected in the internal lamina of arteries [70]. It was found that the presence of elastin contributed to the alignment of collagen fibers, similar to the native extracellular matrix [70]. In the anatomy of native blood vessels, there is a layer of smooth muscle cells for elasticity and contractility. This layer was distinctively facilitated by the presence of elastin in the TEVG [70, 71]. Contractile markers and phenotypical expression of SMC were upregulated via the inclusion of elastin in the TEVG [71]. Despite its influence in the initiation of aortic morphogenesis and the prevention of intimal hyperplasia in native tissues, elastin has not been used routinely in biomedical research due to its limited resources, high expense, and batch-to-batch variations [44, 72].

Chitosan is the second most used biomaterial in vascular tissue engineering. It is a cationic glucose-based homopolymer that is derived from the exoskeleton of arthropods (the alkaline deacetylation of chitin yields chitosan). With the structural advantage of being a polycation, chitosan can interact with the anionic molecule heparin to expedite antithrombotic strategies in the lumen of TEVGs. Chitosan has tunable porosity, low toxicity, and better mechanical properties than many natural polymers. Chitosan scaffolds inhibit inflammation after implantation, modify viability chemically, and have high affinity with in vivo macromolecules [20]. Chitosan exhibits a structure similar to glycosaminoglycans (GAGs) – a component of the ECM. GAGs and GAG-based materials are projected to be important in the regeneration of vascular tissue due to their inhibitory effects on vascular smooth muscle cells and anticoagulant properties [73]. In vivo, TEVGs with the addition of chitosan have been shown to display similar mechanical properties as the native vessels [74,75] and the grafts remained patent after six months of implantation [74].

Upon cell infiltration, chitosan grafts experienced a smooth intima, regular endocardium, and organized vessel wall [75].

Alginate is an anionic polysaccharide composed of α-L-guluronate (G constituent) and β-D-mannuronate (M constituent). It is the second most abundant natural polymer on Earth. Originating from brown algae, alginate can go through ionotropic gelation in the presence of bivalent ions such as Ca^{2+} and Ba^{2+}. The ratio of M and G residues effectuates different gel properties, with G domains having a higher Young's modulus and thus higher brittleness. The advantages of alginate are low toxicity, low immunogenicity (resisting short-term FBR and long-term inflammation), and selective permeability (as proven in [76]). The main disadvantage of alginate does not contain cell-adhesive peptide motifs. Alginate is mostly used as a hydrogel for microencapsulation and transplantation of cells, rather than as part of the polymer blends for bioprinting, electrospinning, or solvent-casting processes. In [77], alginate-based hydrogel constructs with tubular shapes demonstrate acceptable biological performance in vitro.

Chapter 2 Drug-Eluting Vascular Grafts for Post-Transplant Immunotherapy

2.1 Background Information

2.1.1 Research Motivations

According to the Health Resources and Services Administration, as of October 2023, more than 100,000 patients are waiting on the national transplant list. The postoperative complications including sepsis, infarction, rejection, fibrosis, and graft failure persist in present times, despite the upsurge in the transplant survival percentage. In consequence, physicians have prescribed to their patients a structured regime of antibacterial and immunosuppressant medications to curtail the

aforementioned risks. The list of medications requires absolute compliance from organ recipients to effectively maintain their postoperative well-being. Nevertheless, in an observational study of kidney recipients [78], almost half (48%) of the death-censored graft failures beyond two years are associated with medical noncompliance. A significant proportion of these failures (68%) are patients younger than 50 years old. It was conclusively shown that adverse effects on the autograft were caused simply by patients taking less than the recommended amount (because of financial concerns), taking the dose at inconsistent hours, or missing a dose of immunosuppressants [79]. Immunosuppressant is a class of medications that does not relent negligence or forgetfulness. This incidence portrays the first impediment following organ transplantation: to assuage the severity of immunosuppressant nonadherence, especially in pediatric recipients.

Graft rejection is an immunological response that is primarily mediated by the T-cells. Tacrolimus (TAC; also known as FK506) is an FDA-authorized oral medication for the prevention of allogeneic post-organ transplant rejection. Tacrolimus belongs to a category of immunosuppressants known as calcineurin inhibitors. Calcineurin is a protein complex of calmodulin-binding catalytic subunit (calcineurin-A) and calcium-binding regulatory subunit (calcineurin-B). To comprehend the mechanism of action of calcineurin inhibitors, it is essential that T-cell priming be explained. T-cell priming (de novo activation of T-cell responses) requires concurrent activation of two signals on T-cells: recognition of peptides bound to major histocompatibility complex (MHC) molecules through the T-cell receptor (TCR), and CD28 co-stimulation via CD80/CD86 on antigen-presenting cells (APCs) [80]. Calcineurin is thereafter activated by the intracellular calcium release [81]. If tacrolimus selectively binds to immunophilins (a type of cytoplasmic receptor [82]), calcineurin transduction activity is halted. The complex formation between tacrolimus and immunophilins inhibits the translocation of a family of

transcription factors (NF-AT), leading to reduced transcriptional activation of pro-inflammatory cytokine genes for interleukin (IL)-2, tumor necrosis factor (TNF)-α, IL-3, IL-4, CD40L, granulocyte-macrophage colony-stimulating factor, and interferon-gamma (IFN-γ) [83]. If these cytokines are not synthesized, the signals for T-cell proliferation and differentiation are negated. Moreover, tacrolimus has been shown to down-regulate the nuclear factor-κB (NF-κB) pathway and induce apoptosis of activated T cells by activating caspase 3 [82]. In summary, tacrolimus impairs the transcription of interleukin-2 and other cytokines in T lymphocytes, and therewith interfering with T-cell activation, proliferation, and differentiation [84]. Calcineurin inhibitors principally act on helper T-cells, but sometimes also suppressor T-cells and cytotoxic T-cells.

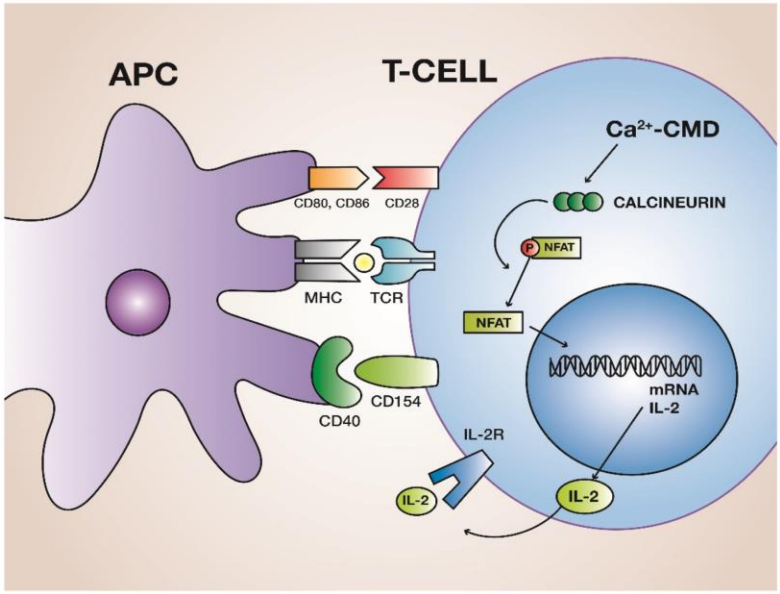

Figure 5. Contact between a peptide of the MHC and the TCR does not activate naïve T-cells due to calcineurin inhibitors blocking IL-2 synthesis [85]

A major disadvantage of oral medication (tacrolimus) is that a considerable proportion of the dosage will lose bioactivity (via intestinal absorption) and bioavailability (via renal filtration) before reaching the site of action (the transplanted organ). If tacrolimus is distributed to the entire

body, global immunosuppression might imperil the patient's health by subjecting them to opportunistic infections (decreased immune activity resulting in increased bacterial infiltration). According to [86], a direct result of prolonged oversuppression is nephrotoxicity and neurotoxicity. Graft failure might additionally be a repercussion of immunosuppressant administration. It could be deduced that the precise concentration of tacrolimus is required for the tissue and organ scales. Thus, a second obstacle presents itself. The delivery of tacrolimus – with exact dosing, at an exact time, to an exact location – is a clinical challenge that could be solved using bioengineering research. Recent advances in the field of drug delivery have attempted to tackle the issue through the innovative use of polymeric [87] or hydrogel [88] encapsulation of the drug as an alternative to systemic administration. These engineering approaches nevertheless require bioengineering expertise to fabricate and employ. Reproducibility is an essential factor if these drug delivery systems are made to satisfy industrial standards and clinical specificities. Tacrolimus must be continuously released into the connecting arteries of the transplanted organ from a robust reservoir. To ensure the highest postoperative compliance among organ recipients, an accessible solution has to be developed and evaluated.

2.1.2 Research Significance

TEVGs have been widely adopted as solutions to several medical conditions, notably congenital vessel abnormalities [89], renal failure [90, 92], alloimmune dysregulation [91], and cardiovascular diseases [93]. In different vascular diseases, different sizes of the grafts are required. A large diameter (>8 mm) and medium to large diameters (6–8 mm) are usually needed for aortic, iliac, and femoral artery repairs, while small-diameter (1–6 mm) vascular grafting is required for coronary artery replacement caused by atherosclerosis or embolism [94]. As a

consensus from medical researchers, small-diameter vascular grafts (SDVG) require further improvements due to frequent stenosis and occlusion in vivo [95].

The encapsulation, immobilization, or dispersion of anti-proliferative, anti-coagulant, or anti-inflammatory molecules into the polymeric matrix can enhance the engineered grafts' biocompatibility [96–100], therefore prompting a potentiality of TEVGs being drug delivery vehicles. For example, antiproliferative paclitaxel release from PCL contributed to the inhibition of SMC proliferation to achieve high patency in vivo [100, 101]. Utilizing a similar concept, this research hereunder investigates a bilayered vascular graft design that synergistically enables the continuous release of tacrolimus to modulate the immunoreactivity at the site of organ transplantation. It is hypothesized that combining the immunosuppression of tacrolimus with biodegradable polymers would yield a drug-eluting vascular graft (DEVG) that could overcome the current limitations in vascular graft engineering. The DEVG is inventive as it provides:

(I) Immunotolerance after transplantation via the local delivery of TAC

(II) Accessibility for patients via the complete mechanical and immunological aid

(III) Individuality for patients via the reproducible and adaptive fabrication process

(IV) Efficiency for physicians via the elimination of secondary surgeries

The DEVG has two layers: (1) the TAC-dispersed inner layer of biodegradable PLCL and PLGA and (2) the supportive outer layer of nondegradable PCU. Using electrospinning, the scaffold could be modified to match the patient's anatomical specificity. To implement immunocompliance for the transplanted organ, the DEVG will be sutured as an anastomosis between the host artery and the donor organ. Tacrolimus can be diffused out of the PLCL/PLGA matrix, into the lumen, and enter the donor organ as the DEVG comes into contact with the circulating blood. The release rate can be controlled by tuning the ratio of PLCL/PLGA co-

monomers. Because the DEVG is the most proximal to the transplanted organ, immunocells in the area will experience the highest concentration of TAC. Off-target effects on other organs will thus subside using this immunosuppressant delivery approach. Supposedly, TAC will be released from the graft for three months (the most critical period of postoperative immunotherapy), so organ acceptance will be maintained at the highest magnitude, regardless of the patient's medical history and habitual behaviors.

The significance of the research is that the DEVG can meet all the design requirements for a TEVG whilst also managing acute and chronic graft rejection following organ transplantation. The rejection of solid organ allografts is the result of a complex series of interactions among innate and adaptive immune effectors, with T-cells being central to this process. Once recipient T-cells become activated, they undergo clonal expansion, differentiate into effector cells, and migrate into the graft where they promote tissue destruction [102]. T-cells, accompanied by other cells like dendritic cells or B-cells, could instigate inflammation and necrosis of allotransplants. Fortunately, with the widespread use of potent immunosuppressive drugs, early graft loss due to acute rejection has decreased dramatically [102]. This is the rationale for the distribution of tacrolimus in a vascular graft for organ transplantation. The easy-to-deploy DEVG could appease the consequences of medical noncompliance in patients, so the cost of personal healthcare for thousands of organ recipients can be reduced. As the synthetic intimal layer is completely biodegradable, the DEVG does not require secondary surgery to remove the graft from the patient. This biodegradable layer also allows gradual endothelization, which is crucial in the healing process. Healthy endothelial linings express antiplatelet and anticoagulant agents that prevent platelet aggregation and fibrin formation [103]. The DEVG is fabricated using electrospinning. This is a traditional tissue engineering approach for tubular structures that can be modified to make

scaffolds of different diameters, thicknesses, drug concentrations, and smoothness. All of these adjustable parameters could lead to an individualized product that is adaptable to any patient during post-transplant immunotherapy.

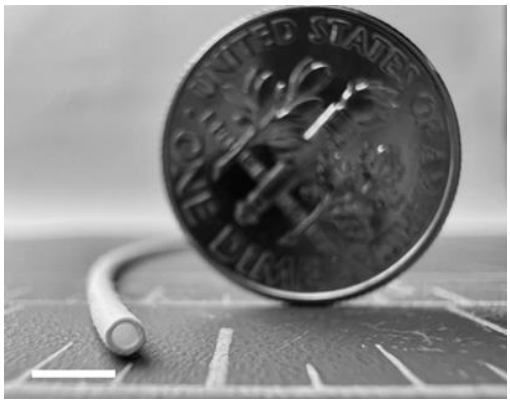

Figure 6. Electrospun DEVG is compared to a dime. The diameter of the DEVG can be tuned during electrospinning. The scale bar denotes a length scale of 5 mm.

For the first time, synthetic vascular grafts are engineered as drug reservoirs for the immunomodulation of T-cells at the allotransplant. DEVGs might instigate a translational breakthrough in postoperative patient care, as the research will conduct in vitro and in vivo experiments on a rodent model for short-term efficacy.

2.2 Experimental Design & Scaffold Fabrication

As indicated in a review study on vascular tissue engineering [20], synthetic polyesters constituted the majority of studied polymers (64%) for TEVGs in the period of 2017–2021. Figure 7 [20] depicts the current biomaterial polymers used in vascular scaffold engineering, and the analysis was based on a title search of "tissue engineering" and "vascular grafts" on the National Institute of Health's PubMed® database. Although natural polymers such as collagen or elastin share more biological resemblance with the adventitia of vascular networks, they are inferior to

synthetic polyesters in mechanical properties, batch-to-batch uniformity, thermodynamic stability, and controllable degradation. Synthetic polymer, despite lacking cell-binding motifs, is thus preferred in this study to minimize variables in the induced-immunomodulation model. If needed, these polyesters could be modified with heparin [70] to enhance the proliferation of EC and inhibit the proliferation of vascular SMC following implantation. With only polyesters in the design, the DEVG also has an ease of handling during the electrospinning and sterilization process. PLGA/PLCL and PCU organic solvents are compatible and the polymers can be simply sterilized under ultraviolet light exposure.

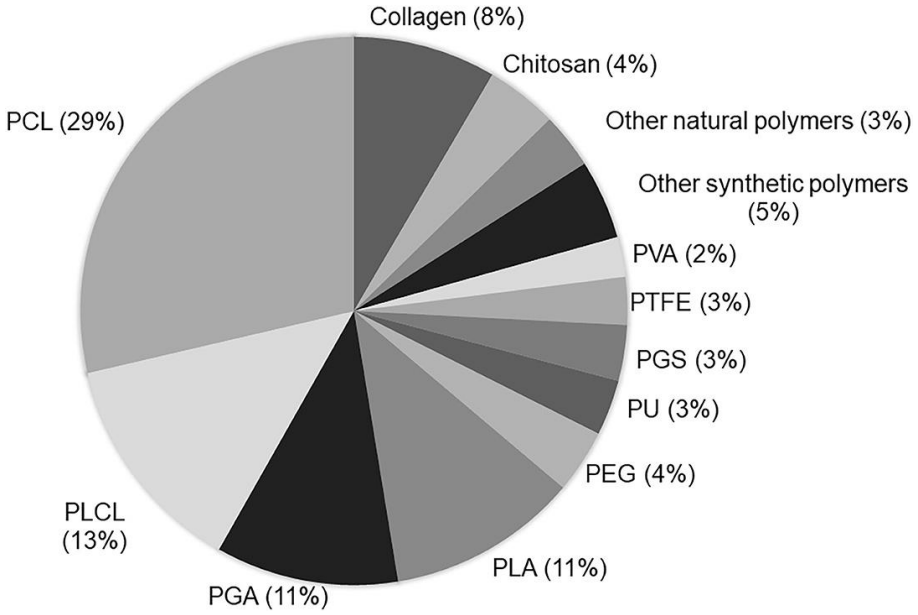

Figure 7. Proportion of Biomaterials Used in Vascular Scaffold Fabrication [20]

The electrospun DEVG is designed to have an inner layer for tacrolimus delivery and an outer layer for mechanical stability. Firstly, the inner of the graft will be fabricated using PLGA/PLCL in 50:50, 35:65, and 20:80 polymer blend composition as experimental groups to find the optimal release kinetics of tacrolimus and mechanical performance. PLCL has been regarded as a suitable polymer for electrospun vascular grafts [59, 60, 62], with appropriate

mechanical and biological properties to facilitate the vascular regeneration process in vivo. PLGA has non-immunogenic degradation products and has been widely used as a platform for drug delivery systems and electrospun tubular scaffolds [104], despite having substandard mechanical properties [105, 106]. Thus, the combined usage of PLGA and PLCL is complementary in terms of mechanical properties and biodegradability. Moreover, PLGA-based grafts have been proven capable of retaining their patency for up to a year [56, 57]. With the initial goal of medicating tacrolimus for three months post-transplantation, this polymer selection can functionalize the sustained delivery of the drug. Secondly, the outer layer of the DEVG is fabricated using PCU. PCU can provide additional mechanical support for the scaffold, specifically to ensure adequate tensile strength, bursting strength, and suture retention strength of the graft.

Tacrolimus (FK506) was purchased in powder form and dissolved in ethanol before mixing with the PLGA/PLCL solution. Poly(D,L-lactide-co-glycolide) (PLGA) was dissolved using hexafluoroisopropanol (HFP) and poly(L-lactide-co-ε-caprolactone) (PLCL) was dissolved using dimethylformamide (DMF). The solubility of tacrolimus in water ranges from 4–12 μg/ml [107], so it was dissolved in ethanol (solubility at 30mg/ml in ethanol) instead. Another reason for water not being used as a solvent is that it may interfere with fiber density and distribution during electrospinning. For the sustained release of a hydrophobic drug to be optimal, it must be entrapped in a biodegradable polymeric system [87, 108]. The direct mixture of TAC solution in the PLGA/PLCL solution was deemed the most simple and favorable approach for electrospinning. Polymer dissolution and drug loading were done with the following protocol:

(I) 2.5 g of PCU (purchased from DSM Biomedical, PA, USA) was dissolved in 15.0 ml of DMF (purchased from Sigma–Aldrich, MO, USA). The PCU volume used for electrospinning the outer layer of DEVG was 3.75 ml.

(II) 50:50 PLGA:PLCL electrospinning solution was made via the addition of 750 mg of powder PLGA (50:50 lactide:glycolide, purchased from Sigma–Aldrich, MO, USA) and 750 mg of powder PLCL (ester terminated, 70:30 lactide:caprolactone, purchased from Sigma–Aldrich, MO, USA) into 10 ml of HFP (assay > 99%, boiling point = 59 °C, purchased from Sigma–Aldrich, MO, USA). This was the inner layer that was thereupon loaded with TAC.

(III) 35:65 PLGA:PLCL electrospinning solution was made via the addition of 525 mg of powder PLGA and 975 mg of powder PLCL into 10 ml of HFP.

(IV) 20:80 PLGA:PLCL electrospinning solution was made via the addition of 300 mg of powder PLGA and 1200 mg of powder PLCL into 10 ml of HFP.

(V) After the polyester solution was made with one of the three ratios, crystalline TAC (assay >98%, chemical formula: $C_{44}H_{69}NO_{12}$, purchased from Avantor, PA, USA) was dissolved into the polymer solution. Briefly, 185 mg of TAC were dissolved in 500 μl of HFP at room temperature, and the mixture was combined with 7.50 ml (not the entire 10.0 ml stock solution) of previously made PLCL/PLGA solution. This would result in a TAC concentration of approximately 23.1 mg/ml for the whole inner layer solution. The collecting rod was approximately 23 cm in length and 1.5 mm in diameter, so each cut DEVG sample of 1 cm would have a drug loading concentration of 1 mg/graft. This was the standard concentration that was used for most in vitro experiments, and a similar scaling method was adopted for 10 mg/graft and 20 mg/graft samples. For in vivo experiments, the loading concentration was approximately 1.4 ± 0.2 mg/graft.

Electrospinning is a traditional method of fabricating biomaterials of tubular shapes with controlled diameter, alignment, and porosity. Briefly, as adapted from previous papers [109–111], the equipment for electrospinning consists of a syringe with a needle attached to its tip connected

to an electrode, a hydrostatic pump, and an electrical source [109]. In the syringe, a polymer solution is conditioned and through the hydrostatic pump, it is directed to a collecting plate. When the polymeric solution is released, it is energized by the electrode, which causes a deformation of the drop and, following this, the formation of a conical jet, known as Taylor cone [110]. This jet originates from the solid fibers that are deposited in the collector rod/plate [111].

The electrospinning parameters of these biomaterials will match the established protocol in the laboratory (Becton Dickinson 10-ml storing syringe, 21G needle, 17 kV voltage, 55–65% humidity, injection speed of 900–1200 μl/hr, and a collection distance of 10cm). The inner layer was fabricated with 7.5 ml of PLGA/PLCL/TAC in HFP solution and the outer layer was fabricated with 3.5 ml of PCU in DMF. The final graft will have a desired thickness and length of approximately 400–600 μm and 1.0 cm, respectively. The entire fabrication process would be in 4–6 hours. After the fabrication process, the drug-loaded graft should be stored at 4°C to minimize further tacrolimus hydrolytic degradation. Tacrolimus degradation during the electrospinning process is unavoidable since humidity is correlated with fiber strength and orientation. If the fabrication happens at a humidity devoid of water vapor, the structural integrity of the collected product will not be maintained.

The overall scheme of the experimental approach is depicted in Figure 8, with the two main phases of in vitro and in vivo characterization of the DEVGs. The anatomical target for the vascular scaffold to replace is the femoral artery of rats, with an ambition to correlate to a kidney transplant model. As conveyed elsewhere in the thesis, the DEVG will serve as a bridge to deliver tacrolimus from the donor organ to, hopefully only, the recipient artery.

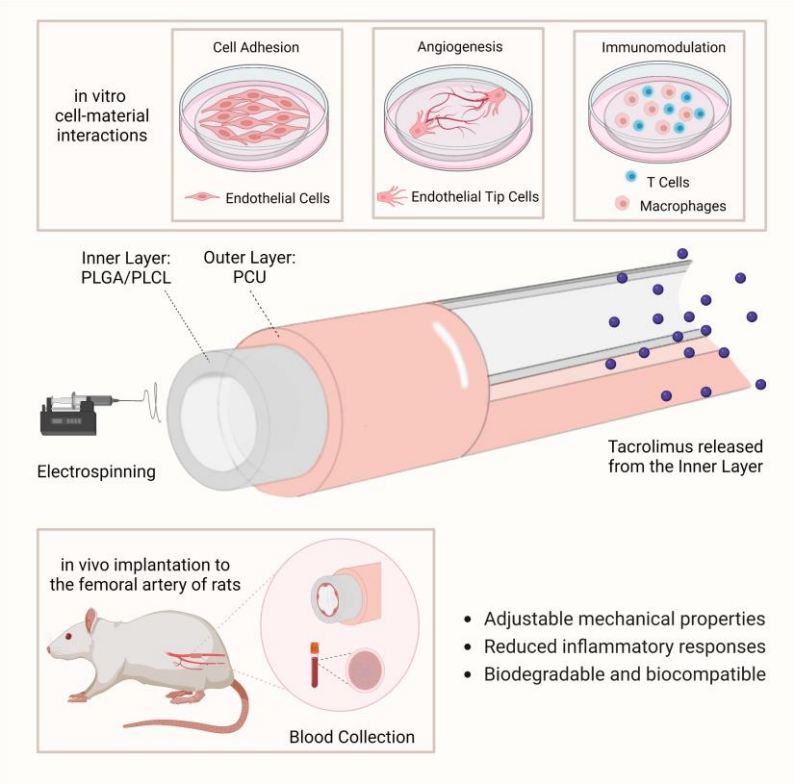

Figure 8. Conceptual Schematic of the Experiments

Chapter 3 Protocols for the Evaluation of DEVG

3.1 Mechanical Characterization

Mechanical testing for elastic modulus, axial tensile strength, axial suture retention strength, and circumferential tensile strength was done using the Q800 Dynamic Mechanical Analyzer (TA Instruments, DE, USA) under tensile deformation in the controlled ramp force mode (rate: 0.05 N/min and preload force: 0.001N) until failure (>50% elongation). This mechanical assessment was similar to the previously described in [112]. The test was performed on a two-centimeter sample of the DEVG (with both layers) after it had been preserved for 24–72 hours after electrospinning. The experiment was done in triplication.

3.2 Hydrolytic Degradation & Drug Release

Three experimental groups of DEVG were conceived, as the inner layer composition of PLGA:PLCL was 20:80, 35:65, and 50:50. All of these inner layers were loaded with TAC. After the DEVG was fabricated, it was simulated with the hydrodynamic conditions matching the native vessels. An in vitro closed-loop tubular system consisting of a test section, sampling ports, silicone rubber tubing, and a roller pump with the compressed section gap set to barely occlusive conditions as described previously was used to examine the degradation and drug release profile of DEVG [113]. Briefly, each sample would be in a circulation loop with Phosphate Buffer Saline (PBS) at 37°C with a renal flow rate matching biological systems (to mimic renal clearance). To obtain the polymer degradation and drug release profile of each group, retained samples from the circulation loop were collected every day for up to three months. Sample weight and pH changes were recorded. The detection of TAC at such a minimal amount needed to be done with an Enzyme-Linked Immunosorbent Assay (ELISA) detection kit (PRO-Trac II Tacrolimus ELISA kit, DiaSorin, MN, USA). PLGA/PLCL degradation and released TAC data were plotted as a function of time.

3.3 Scanning Electron Microscopy

The micromorphology of the electrospun surface of DEVG will be imaged by Scanning Electron Microscopy (SEM), with a gold coating on 1-centimeter square samples. The scanning was done with an established protocol at the California NanoSystems Institute to visualize the effect of fiber composition at different ratios of PLGA and PLCL. The fiber diameters, porosity, and interconnectivity will be measured from the images using the ImageJ software (developed by the National Institute of Health, NY, USA).

3.4 In Vitro Cellular Interactions

3.4.1 Endothelial Cell Adhesion

To prove that our scaffold can perform as a biocompatible matrix, the adhesion of endothelial cells to the inner layer was tested. A mouse cell line, bEND3, will be used for the assay. bEND3 are endothelial cells isolated from brain tissue derived from a mouse with endothelioma (purchased from ATCC, VA, USA). bEND3 (10–18th passage) was cultured in standard Dulbecco's Modified Eagle Medium (DMEM) for 24 hours with the DEVG in the microplate. The DEVG in the culture microplate was of increasing concentrations of tacrolimus (0 mg/graft, 1 mg/graft, 10 mg/graft, and 20 mg/graft). The bEND3 seeding density was 30,000–50,000 cells per well in the microplate. Immunostaining with 4′,6-diamidino-2-phenylindole (DAPI; purchased from Thermo Fisher Scientific, MA, USA), and phalloidin was performed after 24 hours of incubation. Images are captured using Fluorescent Microscopy (Zeiss, Baden-Württemberg, Germany) and the number of adherent cells is quantified by ImageJ.

3.4.2 Endothelial Cell Angiogenesis

The optimal concentration of tacrolimus should be identified with in vitro experiments on endothelial cells. A study in 2018 [114] investigated the cytotoxic effect of TAC on other cell types, most notably endothelial cells. The study proved that the cytotoxic effect of tacrolimus was dose-dependent, and their primary effects on endothelial cells were spheroid disaggregation and tubulo-angiogenesis retardation. Should the released concentrations of tacrolimus exceed 18 ng/ml per 24 hours, undesirable off-target effects on the nearby endothelium would occur.

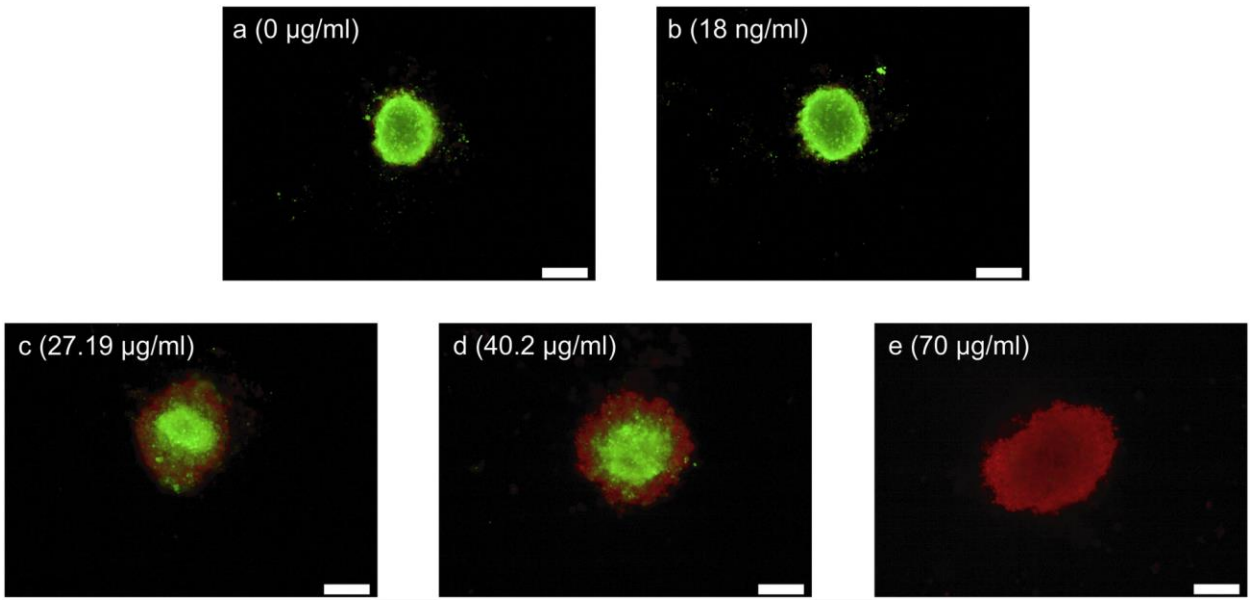

Figure 9. Live (green)/dead (red) staining of HUVEC spheroids treated with different tacrolimus concentrations (a–e) for 24 h. The figure was adapted from [114].

For the experiment, a 48-well microplate was coated with roughly 100 µl of matrigel with centrifugation to ensure a uniform distribution at the bottom of each well. The study should be conducted with HUVECS (purchased from ATCC, VA, USA) of no more than the 10^{th} passage. The DEVG of varying loading concentrations of tacrolimus (0 mg/graft, 1 mg/graft, 10 mg/graft, and 20 mg/graft) were co-cultured on top of the matrigel surface. Incubation was done for 72 hours for the differentiation of the HUVECs. Matrigel induces endothelial cells to differentiate as evidenced by both the morphologic changes and by the reduction in proliferation; ergo, it offers a convenient model to study biochemical and molecular events associated with angiogenesis [115]. After this, the samples were characterized using Brightfield Microscopy (Zeiss, Baden-Württemberg, Germany).

3.4.3 Macrophage Activation

After a non-native material is implanted into the body, neutrophils will be recruited to start the phagocytosis of the biomaterial. This initial response is followed by infiltration of circulating monocytes, which mature into highly phagocytic macrophages that phagocytose dying neutrophils and pathogens, clear up cellular debris, and secrete soluble factors [116]. Early in the inflammatory cascade, macrophages secrete pro-inflammatory factors that orchestrate and support the killing response. As the threat is cleared, they transition to an anti-inflammatory phenotype, which is associated with the promotion of tissue repair and, eventually, the resolution of inflammation [116–118]. The notable pro-inflammatory and anti-inflammatory cytokines are presented as follows.

Tumor necrosis factor (formerly known as TNF-α) is a 185-aminoacid glycoprotein initially described for its ability to induce necrosis in certain tumors. It stimulates the acute phase of the immune response. This potent pyrogenic cytokine is one of the first to be released in response to a pathogen and can exert its effects on many organs. TNF induces vasodilation and loss of vascular permeability, which is propitious for lymphocyte, neutrophil, and monocyte infiltration [119, 120]. Concomitantly, the gene for nitric oxide synthase 2 (NOS2) is upregulated during inflammation. This is an inducible enzyme that has been associated with M1 macrophage promotion in the inflammatory phase [121]. Interleukine-1 (IL-1) is also a class of pro-inflammatory mediators. Three forms of IL-1 are known: IL-1α, IL-1β and IL-1Ra. Similar to TNF, IL-1β is an endogenous pyrogen that is produced and released at the early stages of the immune response to infections, lesions, and stress. During inflammation, IL-1β stimulates liver-derived proteins, induces a systemic fever, triggers prostaglandin secretion, elicits vasodilation and

localized inflammation through histamine release, and enhances the differentiation of CD4+ T-cells [119, 122].

In stark contrast, IL-10 is a 35 kD macrophage-secreted cytokine that inhibits the inflammation cascade. Its main potency concerns the suppression of macrophage activation and production of TNF, IL-1β, IL-6, IL-8, and IL-12. Furthermore, IL-10 also suppresses MHC-II expression in activated macrophages and is thus a potent inhibitor of antigen presentation [119, 123]. IL-10 also has an anti-inflammatory effect on eosinophils, basophils, and mast cells.

It is rendered necessary to scope the effect of released tacrolimus on a potent mediator of innate immunity and a major antigen-presenting cell type: the macrophages. By surveying the number of cytokines released by primary macrophages on the DEVG, an insight into the graft's ability to modulate the acute phase of inflammation can be obtained. Peritoneal monocytes from albino rats were harvested by peritoneal lavage four days after intraperitoneal injection of thioglycollate (3% w/v). After being differentiated with the addition of macrophage colony-stimulating factor (M-CSF) and activated with lipopolysaccharide (LPS), the induced macrophages were co-cultured with loaded-and-sterilized DEVG with increasing concentrations of tacrolimus. The seeding density of macrophages will be approximately 100,000 cells per well in the microplate. Quantitative Polymerase Chain Reaction (qPCR) tests for mRNA expression of inflammatory (NOS2, TNF-α, IL-1β) and anti-inflammatory (IL-10) cytokines were conducted.

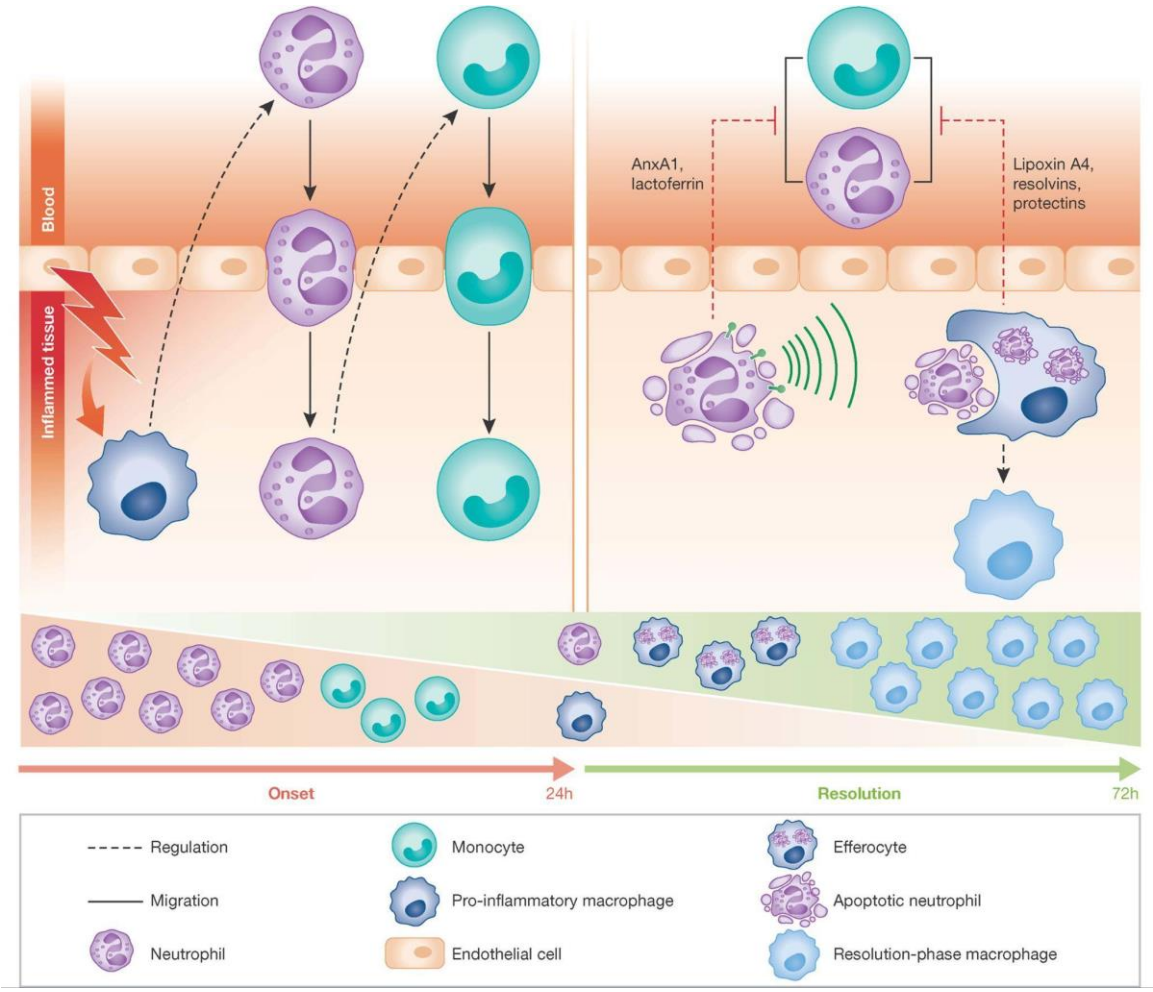

Figure 10. Cellular Interplay During the Resolution of Inflammation. During early phases of inflammation, tissue-resident cells sense damage and launch the release of signals that induce rapid neutrophil and delayed monocyte emigration. Resolution is initiated when neutrophils become apoptotic thus secreting mediators that inhibit continued neutrophil infiltration. Ingestion of apoptotic neutrophils changes the macrophage phenotype towards a resolution-phase macrophage, which promotes return to tissue homeostasis. Figure 10 was adapted from Ortega-Gómez et al [124].

3.4.4 T-Cell Proliferation

The effect of released tacrolimus on T-cell proliferation was done according to established protocols in the literature [125]. Briefly, after the splenic extraction of the cell clusters, murine

splenocytes were isolated from naive T cells. T-cells were then labeled with the CellTrace™ CFSE Cell Proliferation Kit (Thermo Fisher Scientific, MA, USA). Carboxyfluorescein succinimidyl ester (CSFE) is an amine-reactive dye that becomes fluorescent upon hydrolysis by cytoplasmic enzymes. The CSFE fluorescence can be retained inside the cell and measured by flow cytometric analysis. After the media (RPMI 1640 basal medium supplemented with 10% fetal bovine serum (FBS) was used to dilute CSFE according to the manufacturer's directions, the microplates containing DEVG of varying TAC concentrations were cultured with a T-cell seeding density of 200,000 cells per well for 72 hours.

3.4.5 T-Cell Activation

Primary naive T lymphocytes of splenic source can be used for the T-cell activation assay with an analogous procedure. The activation assay was also performed in 24-well microplates with a seeding density of 200,000 cells per well. The samples in this experiment were free-flowing cells without graft (sample A), cells with a negative control graft (0 mg/graft) (B), and cells with DEVG of increasing TAC concentrations [0.01 mg/graft (C), 1 mg/graft (D), 10 mg/graft (E), and 20 mg/graft (F)]. T lymphocytes, following standard purification protocol (EasySep™ Magnet; purchased from Stem Cell Technologies, BC, Canada) will be activated using Dynabeads™ Human T-Activator CD3/CD28 for T Cell Expansion and Activation kit (Thermo Fisher Scientific, MA, USA) and IL-2 (an activator of T-cells). Each well should have 5 µl Dynabeads™ and 1 µl IL-2. The incubation period will be 72 hours and the results will be quantified using fluorescence-assisted cell sorting (FACS) for CD69 (an activation-inducing molecule that is transiently expressed on T-cells in early events of activation) and CD25 (the low-affinity IL-2 receptor α-chain that is expressed on activated T-cells).

3.5 In Vivo Tissue Interactions

3.5.1 Vascular Graft Implantation

Sprague–Dawley rats at 6–8 weeks old (weighing 200–300g) were chosen as the experimental subjects of the in vivo study. The rats were administered Isoflurane, an inhalational anesthetic, for 5–10 minutes before the surgery was conducted. The dose of Isoflurane was 4–5% for induction and 1–3% for maintenance of anesthesia. After being anesthetized, the rats were monitored for physiological parameters such as body temperature at 35.8–37.5°C, oxygen saturation at >95%, and heart rate of 300–550 beats per minute. During the surgery, the rats were placed at the supine position, with the exposure of the femoral artery. The longitudinal incision was performed around the superficial femoral artery. Specifically, the surgeons made a skin incision with the scalpel designed for this animal. The fascia layer of the rat thigh area was then identified and incised, prior to the dissection of the superficial femoral artery. After the meticulous dissection of the femoral artery, the surgeons acquired a tissue sample of 1.0–1.5 cm. The loading concentration was 1.4 ± 0.2 mg TAC per 1 cm DEVG sample. The DEVG, which was sterilized for 24 hours under UV irradiation, was prepared to replace this native artery (1.0–1.5 cm in length and 0.4–0.6 mm in lumen diameter). The DEVG was soaked in heparin/saline solution (1:500 dilution) for several seconds. Subsequently, vessel anastomosis was performed at the site of the incision with the assistance of a microscope. The suture in use was 10–0 monofilament nylon suture. After the procedure, circulation and patency at the inserted vessel position were checked by manual compression. The fascia of the thigh area was afterward repaired with the 5–0 Dexon absorbable suture (PGA-based suture with PGCL coating). The skin was closed with a 4–0 monofilament nylon suture. After muscular and neurologic assessment during the anesthesia

recovery period, the rats were transferred to postoperative care at the Division of Laboratory Animal Medicine (DLAM).

3.5.2 Venous Blood Collection

A recent study has proven the maintenance of tacrolimus concentration in blood at 10.15–11.55 ng/ml for four weeks after transplantation significantly reduces the risk of acute and chronic graft-versus-host diseases (GVHD) without increasing relapse rate, while a concentration higher than 11.00 ng/ml during the first-week post-transplantation may be associated with suppressed graft-versus-tumor effect and higher relapse rate [126]. The importance of maintaining the therapeutic window of tacrolimus in the blood serum was therefore established. As an immunosuppressant of cytotoxic and regulatory T-cells and prophylaxis of GVHD, tacrolimus must be released at the proper concentration to potentiate its potency. The serum concentration of tacrolimus in each experimental group would be determined weekly during the 30 days after implantation. Initially, the whole blood was extracted from the rat's tail vein using a 24G needle. Each week roughly 400–500 µl of blood was drawn from the rat. The collecting vials were subsequently allowed to form clots at room temperature for 30 minutes. The clots could be removed by centrifuging at 2000g (~4000 rpm) for 15 minutes in a refrigerated centrifuge. Only 100 µl of serum could be collected at the end and the concentration of tacrolimus in the sample was calculated using the PRO-Trac II Tacrolimus ELISA kit.

3.5.3 Arterial Ultrasound Imaging

Although synthetic grafts offer off-the-shelf availability and minimal donor-site morbidity [98], they often experience occlusion (thrombogenesis) or stenosis (intimal hyperplasia) after

being implanted. Patency is regarded as a major impediment of small-caliber synthetic vascular grafts in clinical applications, while in comparison biologically-originated grafts (isografts, autografts, allografts, or xenografts) possess a much higher patency rate. By engineering the surface chemistry and spatial geometry of TEVGs [127, 128], researchers have achieved preclinical success in improving the patency of synthetic grafts.

The design of an integrated drug delivery and tissue engineering system such as the DEVG must similarly be challenged by in vivo assessment, the simplest parameter of which is patency. Immediately following implantation and over four weeks, directional color Doppler ultrasonography (Acuson Cypress, Siemens Medical Solutions, CA, USA) was routinely conducted at the femoral anastomosis. DEVG's lumen diameter and blood flow velocities were recorded while the rodent subjects were under anesthesia. Physiological parameters were monitored during the patency examination.

Chapter 4 Results for the Evaluation of DEVG

4.1 Mechanical Characterization

After the DEVG was electrospun, the sample was left untouched for 24–72 hours to ensure the complete vaporization of organic solvents (HFP and DMF). Figure 11A/B illustrates the circumferential/longitudinal deformation of the DEVG at various inner layer compositions: 20:80 PLGA:PLCL, 35:65 PLGA:PLCL, and 50:50 PLGA:PLCL. The outer layer of PCU remained constant in thickness and composition for all these DEVG samples and all experiments in this research were done with bilayer DEVGs. Young's modulus of elasticity was calculated by diving engineering stress (σ) with strain (ε). The data beyond the elastic region (>6–10% strain) was

omitted since the graft was designed to retain its shape (satisfying compliance requirements) when cyclic flow was established in humans. For circumferential deformation testing, the modulus of 20:80 PLGA:PLCL, 35:65 PLGA:PLCL, and 50:50 PLGA:PLCL DEVG samples were respectively 16.9 MPa, 13.7 MPa, and 9.3 MPa. For longitudinal deformation testing, the DEVG modulus of 20:80 PLGA:PLCL, 35:65 PLGA:PLCL, and 50:50 PLGA:PLCL DEVG samples were respectively 36.6 MPa, 39.1 MPa, and 44.2 MPa. It was observed that the addition of PLGA (specifically lactide moieties) increased the rigidity of PLCL, which was consistent with the results of [129]. From Figures 11A and 11B, it could also be concluded that 50:50 PLGA:PLCL samples presented the highest resistance to bidirectional deformation.

According to the manufacturer of 80A Bionate® PCU, the polymer has a flexural modulus of 28.7 MPa, ultimate elongation of 531%, tear strength of 41.8 N/m, and water absorption of 1.2%. The human arteries were estimated to have a modulus of 1.4 MPa (femoral), 2.3 MPa (iliac), and 1.24 MPa (carotid) at physiologic blood pressure of 80–120 mmHg [130]. In comparison to the native arteries, the DEVG exhibits a much higher stiffness. The surplus amount of combined PLGA/PLCL and PCU stiffness is advantageous because over time the inner layer will degrade and hence only the PCU is left in the biological system. The remaining PCU layer is expected to provide biomechanical support when all of the inner layer is metabolized. PCU has previously been proven to have optimal durability for use as long-term medical implants in humans [34] and rodents [35].

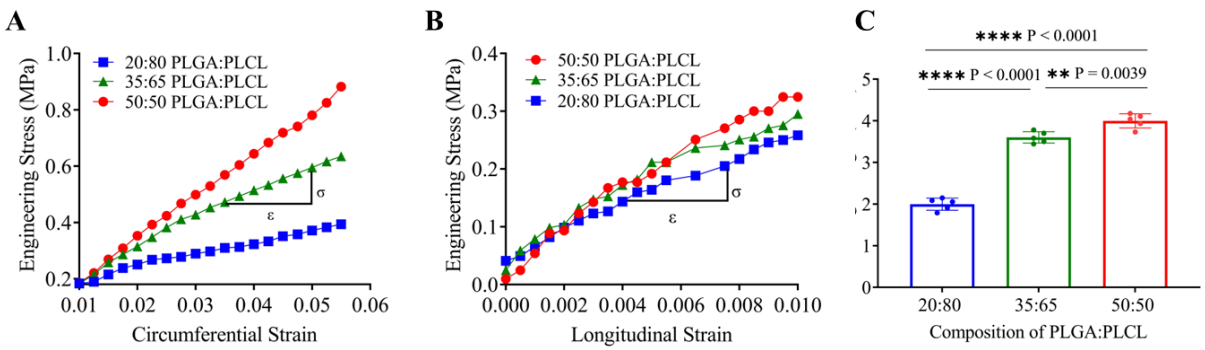

Figure 11. Mechanical Characterization of the DEVG at Varying PLGA/PLCL Composition, with (A): Circumferential Deformation, (B): Longitudinal Deformation, and (C): Suture Retention

Figure 11C shows the breaking strength of these DEVGs, as examined by nylon suture retention as an anastomosis in the middle of the graft. Figure 12 is a schematic representation of the suture retention test adapted from [131]. Under uniaxial deformation, 20:80 PLGA:PLCL had a suture retention strength of 2.0 MPa, which was statistically different from that of 35:65 PLGA:PLCL and 50:50 PLGA: PLCL (3.6 MPa and 4.0 MPa, respectively). This result was comparable to the woven PLLA nanotextile vascular graft engineered by Joseph et al. [132]. In this study, bundles of electrospun PLLA nanofibers were weaved into a nanotextile conduit. The measured suture retention for this conduit was 1.5 MPa, and its successful engraftment increased transmural endothelial ingrowth in a porcine model. The DEVG had a higher suture retention, wherefore promised surgical feasibility in vivo.

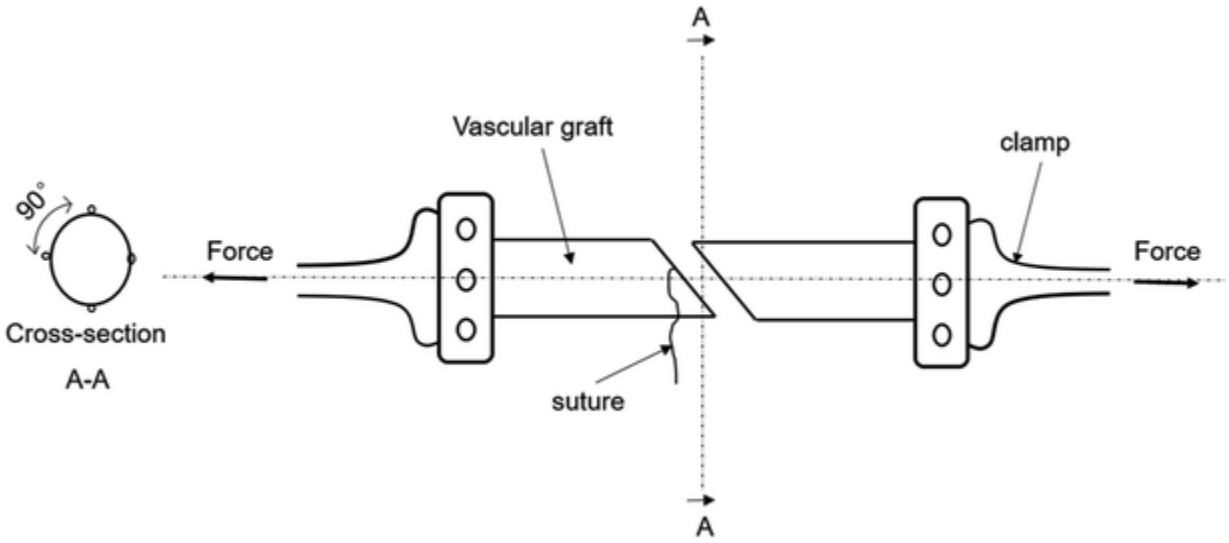

Figure 12. Schematic Representation of the Suture Retention Strength Test [131]

4.2 Hydrolytic Degradation & Drug Release

Figures 13A/B showcase the weight loss and pH changes of the DEVG, influenced by the PLGA/PLCL composition in the scaffold. Mechanical strength, swelling behavior, capacity to undergo hydrolysis, and subsequently biodegradation rate of the polymer are directly influenced by the degree of crystallinity of the PLGA, which is further dependent on the type and molar ratio of the individual monomer components in the copolymer chain. As a rule, higher content of PGA leads to quicker rates of degradation, except for the 50:50 ratio of PLA/PGA, which exhibits the fastest degradation, with higher PGA content leading to increased degradation interval below 50% [133]. The incorporation of 50:50 lactide:glycolide PLGA into the inner layer increased its degradation kinetics, as the sample reached 25.9% weight loss in the 12^{th} week. For the 35:65 and 20:80 samples, the maximum degradation in the 12^{th} week was 16.5% and 7.8%, respectively. This structural hydrolysis was translated into the consequential lactic acid and glycolic acid release to the buffer, marking the pH at roughly 2.50 for the 50:50 and 35:65 samples and pH = 3.40 for the

20:80 samples. The substantial decrease in pH could be attributed to the small volume of physiological buffer used in the experiment, and this decrease would not be as major under the clearance of blood circulation. Additional experiments on local inflammation were done with macrophages in the following section.

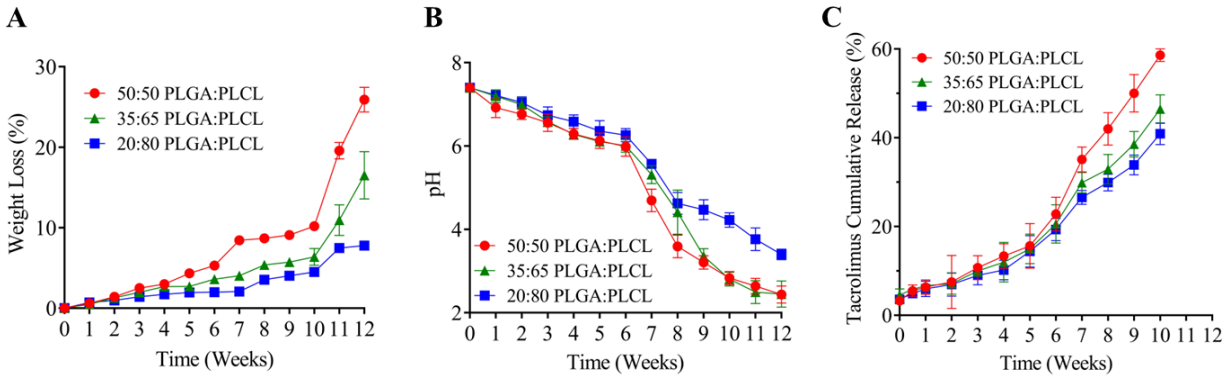

Figure 13. Degradation Behaviors of the DEVG at Varying PLGA/PLCL Composition, with (A): Weight Changes Over Time, (B): pH Changes Over Time, and (C): Tacrolimus Release Kinetics

It might be argued that the selection of 20:80 PLGA:PLCL as the composition for the inner layer was more advisable due to its minimal effects on the pH microenvironment. Nevertheless, the release of tacrolimus from the 50:50 matrix was more appropriate for the intended TAC maintenance and exhibited more mechanical strength per Figure 11. Figure 13C presents the performance of each composition as a drug carrier matrix. At 12 weeks, 60% of the dispersed TAC in the matrix of 50:50 PLGA:PLCL was released. This was similar to the release kinetics of a doxorubicin-loaded PLA-based electrospun vascular graft [43]. The degradation rate of the DEVG was slightly less than that fabricated in [43] primarily due to the addition of caprolactone residues.

4.3 Scanning Electron Microscopy

Significant fiber length changes were discovered in Figure 14 before (A, B. C) and after (D, E, F) hydrolysis occurred. The surface morphology associated with each DEVG composition was scanned, resulting in the analysis of pore diameters using the ImageJ software as Figure 15. The correlation between fiber length and pore size was previously established [134]. It was shown that the pore diameter of the 50:50 sample experienced a reduction from 23.7 μm to 13.9 μm at three months of degradation. The 35:65 and 20:80 samples underwent an insignificant drop in pore diameter, but initially, the distributed nanofibers were not advantageous for cell infiltration (diameter <20 μm). The difference in pore diameters of the two samples was not statistically significant, suggesting that further decreasing PLGA composition had no effect on the pores created.

Increased pore sizes could promote increased cell infiltration and proliferation in the scaffold. Since the electrospinning system was made in-house, it was difficult to control templating patterns. The electrospinning process should aim for the largest pore diameters that could be fabricated from compositional changes. According to surface morphology examination, 50:50 composition was the best option for vascular scaffold fabrication. The 50:50 composition of PLGA/PLCL for the inner layer of the DEVG was deemed the most probable candidate for in vitro and in vivo studies by virtue of the optimal fiber length, pore distribution, degradation kinetics, suture retention, and mechanical elasticity.

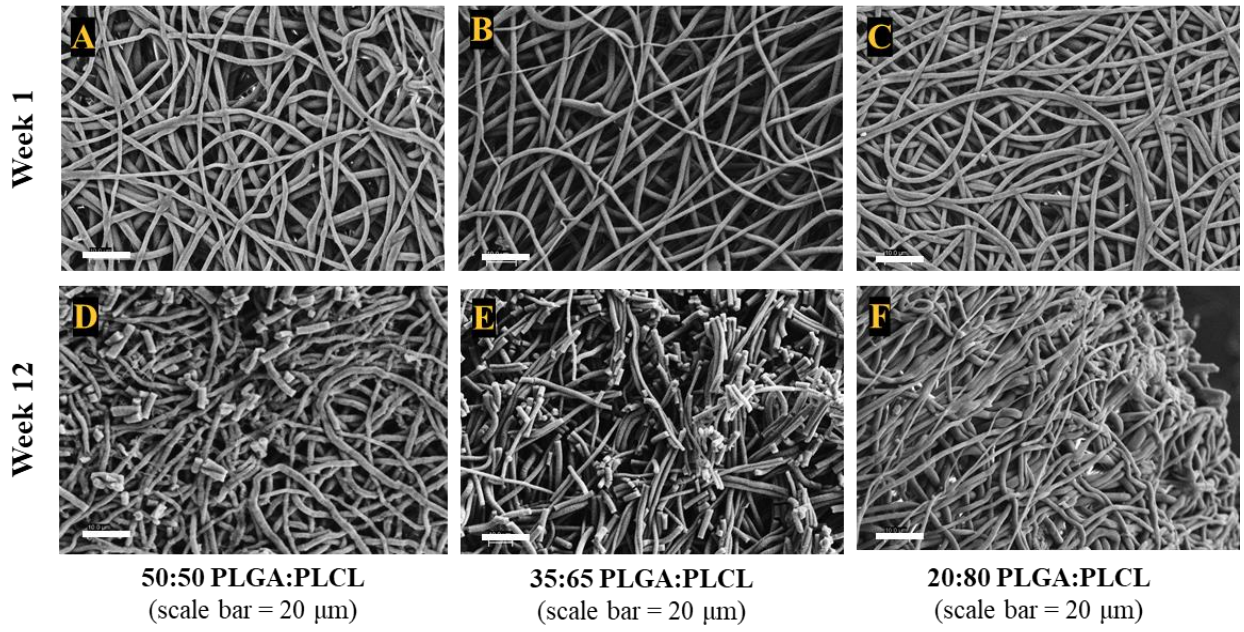

Figure 14. SEM Analysis of the DEVG at Varying PLGA/PLCL Composition in Week 1 (A, B, C) and Week 12 (D, E, F). The scale bar denotes 20 μm.

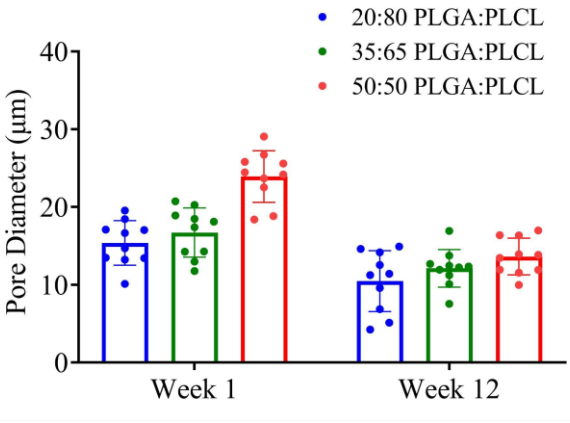

Figure 15. Pore Diameters of the DEVG upon SEM. The image was processed using ImageJ.

4.4 In Vitro Cellular Interactions

4.4.1 Endothelial Cell Adhesion

As mentioned above, starting from this in vitro experiment onwards, all DEVG used would have an inner layer of 50% PLGA and 50% PLCL. The ensuing biocompatibility studies were dedicated to finding the idealistic loading concentration of TAC and evaluating the DEVG's cellular interactions. Figure 16 describes the cellular adhesion and viability of bEND3 mouse cells on the varying TAC loading conditions of 0, 1, 10, and 20 mg/graft. After DAPI (for nuclei) and phalloidin (for actin filaments) staining at 24 hours, the endothelial cell morphologies were as below. Figure 16A and Figure 16B did not have much difference in cell viability, therefore proving the inner layer conductive for cell adhesion. It could also be deduced that the loading of the DEVG at 20 mg TAC/graft was cytotoxic to the survival of the endothelial cells from Figure 16D.

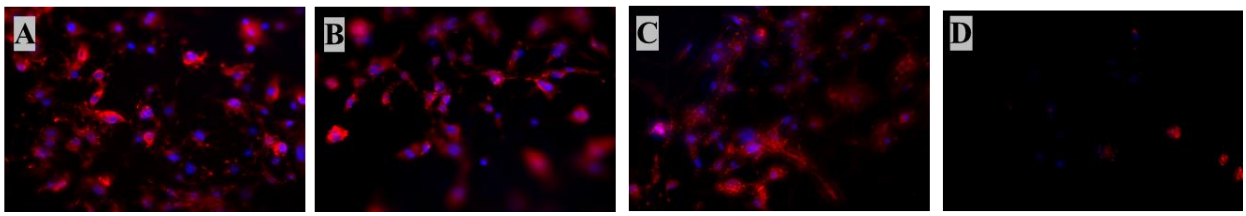

Figure 16. Fluorescent Microscopy of Stained bEND3 Cells on DEVG at Varying TAC Loading Concentrations: (A): 0 mg/graft, (B): 1 mg/graft, (C): 10 mg/graft, and (D): 20 mg/graft

4.4.2 Endothelial Cell Angiogenesis

Angiogenesis is the formation of new blood vessels, which is characteristic of the endothelial cells' migration, proliferation, and differentiation capabilities. The angiogenic potential of HUVEC on the DEVG was evaluated via the assistance of matrigel. Figure 17A–D confirmed that serious inhibition and disaggregation of endothelial cells would occur if the TAC loading concentration exceeded 1 mg/graft (or 18 ng/ml/day) in the media. This result was

consistent with that reported in [114]. Quantitative analysis of the angiogenesis assay was done using ImageJ for junctions (Figure 16E), endpoints (Figure 16F), vessel length (Figure 16G), and vessel area (Figure 16H). In general, the more tacrolimus released into the media, the fewer intact vessels and connectional tubes were detected. If the tubes were destroyed during angiogenesis, total junctions would decrease and total endpoints would increase. Apoptosis would be imposed on endothelial cells if the antiproliferative TAC were loaded at 20 mg/graft. Figure 16D depicts cell debris as the aftermath of spheroid disaggregation and destruction. Tacrolimus was concluded to be inauspicious to the proliferation and differentiation of endothelial cells at high concentrations (>40 μg/ml/day).

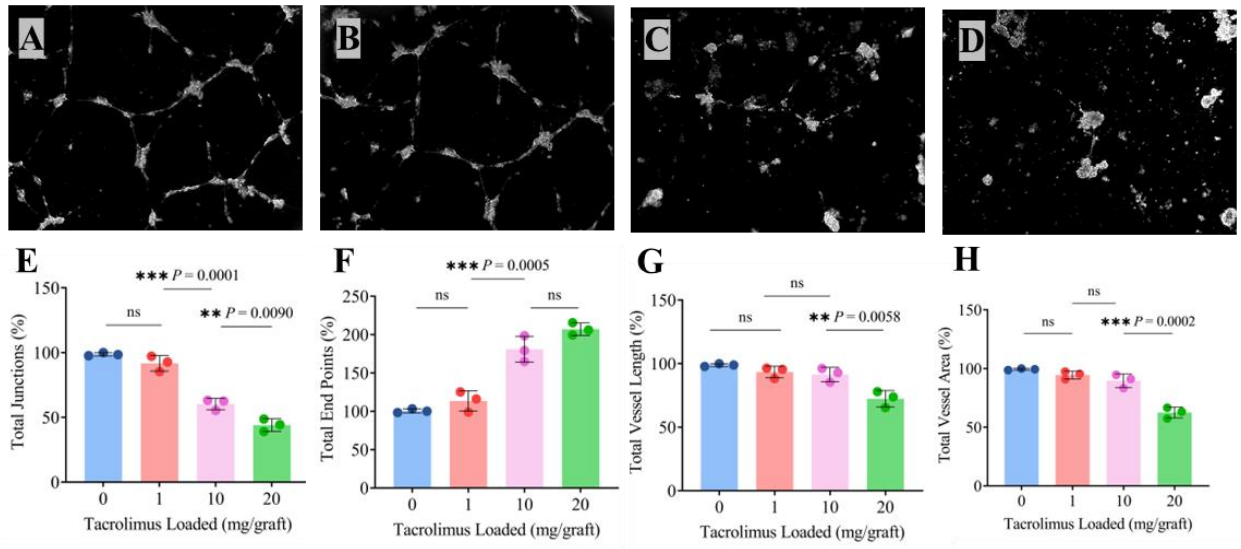

Figure 17. Angiogenesis Assay of HUVECs on DEVG at Varying TAC Loading Concentrations: (A): 0 mg/graft, (B): 1 mg/graft, (C): 10 mg/graft, and (D): 20 mg/graft. The bar graphs depict the quantification of the angiogenic capability of the cells, with (E): Total Junctions (%), (F): Total End Points (%), (G): Total Vessel Length (%), and (H): Total Vessel Area (%) upon TAC Inhibition.

This phenomenon could be referred to as tacrolimus-mediated serine/threonine-specific protein kinase B (abbreviated as PKB or AKT) inhibition [135]. Tacrolimus can abrogate the

phosphorylation of AKT – a multifunctional intracellular regulator of cell growth, metabolism, and survival [135]. Moreover, tacrolimus can also induce endothelial dysfunction through the attenuation of AKT and destruction of angiogenic tubes [136].

4.4.3 Macrophage Activation

Macrophages, the immune cells that are present in most tissues, account for 10% of immune cells but contribute nearly 50% of the total cellular mass due to their large size [137]. The quantification of macrophage cytokine secretion is necessary to determine the immunogenicity of the drug-eluting graft. Figure 18A–C illustrates the relative mRNA expression of pro-inflammatory cytokines TNF-α and IL-1β and inducible genes NOS2. The upregulation of NOS2 and synthesis of TNF-α were inhibited by the released tacrolimus in the media. qPCR revealed the expected downward trend in these expression levels with increasing concentrations of TAC. Interestingly, the production of IL-β increased with TAC of 1 mg/graft and 10 mg/graft but completely zeroed out at 20 mg/graft. A high concentration of TAC might have induced apoptosis on the macrophages, thus no expression of TNF-α, IL-1β, and NOS2 was detected at 20 mg/graft. It was concluded that tacrolimus strongly suppressed LPS-stimulated inflammatory cytokine production from activated macrophage in a dose-dependent manner, which was following the findings of Yoshino et al. [138]. Figure 16D showcases the production of IL-10, an anti-inflammatory cytokine, upon tacrolimus release. The loading concentration of 1 and 10 mg/graft had no noticeable effect on the production of IL-10.

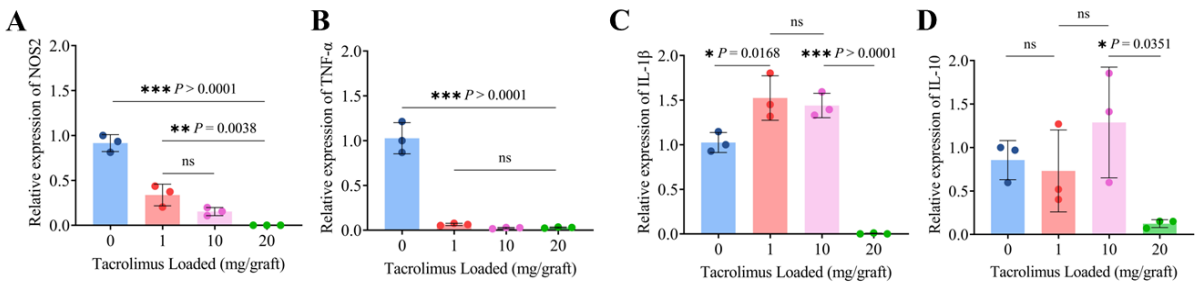

Figure 18. qPCR for the Expression of Pro-Inflammatory and Anti-Inflammatory Cytokines from the Induced Macrophages Upon TAC Release from DEVG: (A): NOS2, (B): TNF-α, (C): IL-1β, (D): IL-10

4.4.4 T-Cell Proliferation

The effect of tacrolimus on T-cell proliferation and activation was well-recognized. Figure 19 demonstrates the FACS analysis of CSFE-stained T-cells when TAC was released from the DEVG. After 72 hours of incubation, the negative control sample witnessed 6 signals of cell division. The 1 mg/graft concentration also shared the same number of fluorescent signals, yet the cell count was significantly less. The 10 mg/graft and 20 mg/graft loading concentrations effectively impeded the division of T-cells to 4 and 2, respectively. It was clear that the more tacrolimus was introduced to the solution, the harder it was for T-cells to divide.

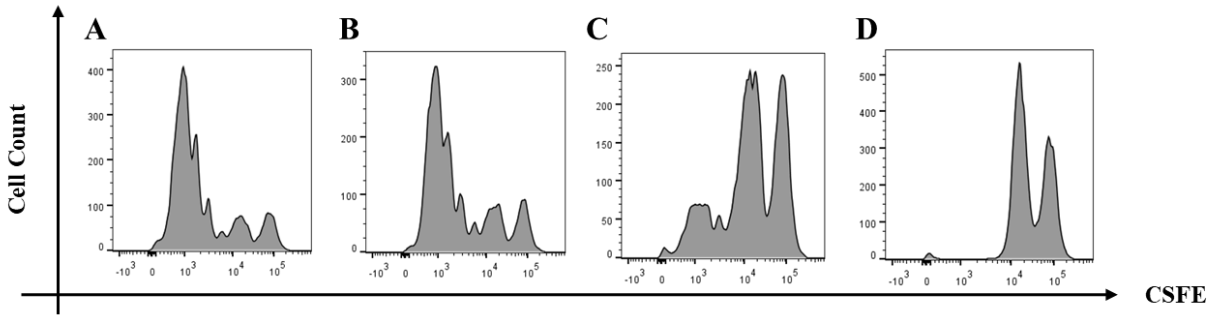

Figure 19. FACS Analysis of the T-Cell Population upon TAC Release from DEVG at Varying TAC Loading Concentrations: (A): 0 mg/graft, (B): 1 mg/graft, (C): 10 mg/graft, and (D): 20 mg/graft

4.4.5 T-Cell Activation

Figure 20A (only T-cells present) and Figure 20B (DEVG of 0 mg/graft) shared similar results in quartile 2 (70.8 versus 69.8). Quartile 2 represents the double-positive region of CD69 and CD25 receptors of the activated T-cells. As mentioned earlier, CD69 is a classical early marker of lymphocyte activation and CD25 is a component of the IL-2 receptor on activated T lymphocytes. 0.01 mg/graft (Figure 20C) was deemed an impotent concentration of TAC as there were no changes to the markers of T-cell activation. Figure 20D–F indicated the inhibition of T-cell inflammatory response via IL-2 synthesis at 1, 10, and 20 mg/graft. Surprisingly, at high concentrations of TAC, a proportion of T-cells still expressed CD69 – an early marker of activation. This might be explained as even during TAC release, T-cells were still able to partially initiate the activation cascade, yet this process was not stable and was abruptly inhibited by the immunomodulator.

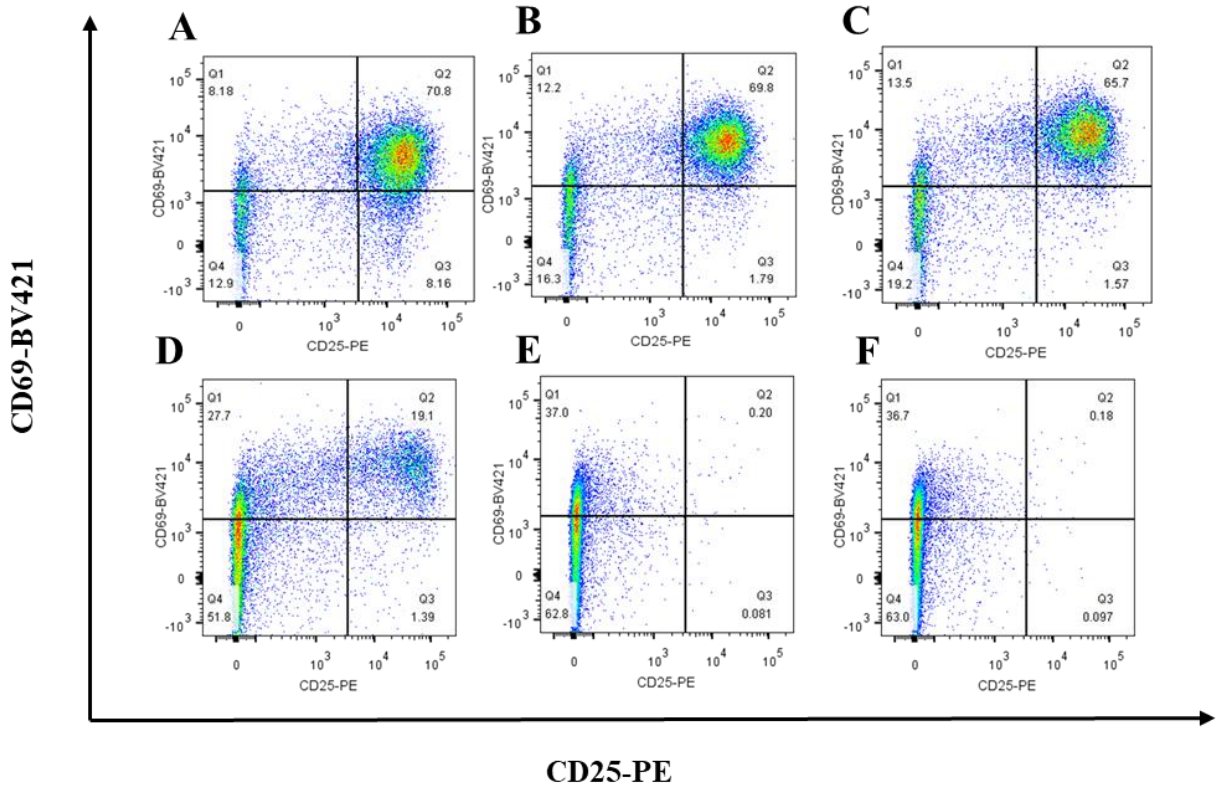

Figure 20. FACS Analysis of T-Cell Activation Markers (CD69 and CD25) upon TAC Release from DEVG at Varying TAC Loading Concentrations: (A): No DEVG, (B), (C), (D), (E), (F): DEVG at 0, 0.01, 1, 10, and 20 mg/graft, respectively

The immunomodulatory effects of TAC would be greater in vitro than in vivo, as red blood cells would capture a great part of TAC in vivo [139]. Thus, for the clinical assessment of the DEVG's performance, a rodent implantation model was employed using the loading concentration of 1–1.5 mg/graft. The concentration was decided based on several cytotoxicity assays above. The inhibition of T-cells must be maintained to reduce transplant rejection while minimizing off-target trauma on endothelial cells and macrophages.

4.5 In Vivo Tissue Interactions

4.5.1 Vascular Graft Implantation

After the successful implantation of the DEVG into a segment of the femoral artery of an eight-week-old Sprague-Dawley rat. The fitted diameter of the graft was 0.50 ± 0.02 mm. Figure 21A/B depicts the before/after implantation condition of the artery. Circulation was established in the left limb and no occlusion was detected at day 0. Under microscopy (Figure 16D), the DEVG was shown to be anastomosed using surgical nylon sutures. The connection was meticulously performed to avoid torsional deformation on the graft. During postoperative care, the closing wound was routinely checked for infection signs and no dietary restrictions were imposed.

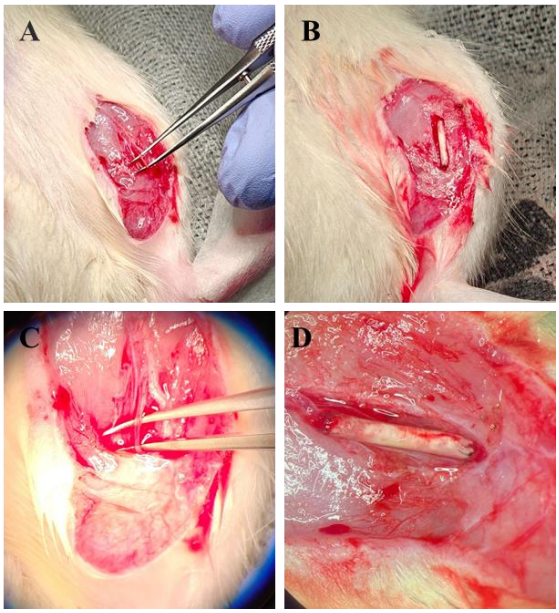

Figure 21. The Implantation of DEVG. (A): The Native Femoral Artery, (B): The Implanted DEVG, (C): The Native Femoral Artery under 10x Microscopy, and (D): The Implanted DEVG under 10x Microscopy

4.5.2 Venous Blood Collection

After the serum was extracted, tacrolimus concentration was determined using ELISA (Figure 22). On average, throughout four weeks, TAC concentration was maintained at 1.0–1.5 ng/ml/day. The cumulative release of TAC at four weeks was only 13.3% of the reservoir per Figure 13C. This number could reach a maximum of 60% at three months after implantation. DEVG was shown to facilitate the local and sustained release of tacrolimus (after an initial burst at days 1–4) in the implanted artery. The immunomodulatory effects of tacrolimus were limited to only the exposed cells in the femoral artery, as the blood sample was collected only in the tail veins of the rat. In future studies, an efficacy comparison between the DEVG and local injections of tacrolimus [141] should be drawn to address the limitations of this therapeutic modality.

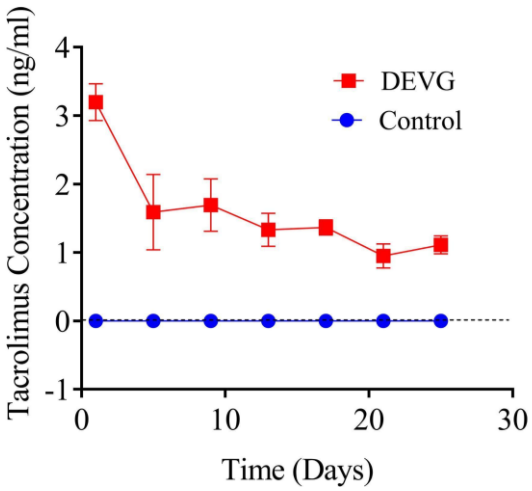

Figure 22. ELISA Detection of TAC in the Blood Serum of Rats

4.5.3 Arterial Ultrasound Imaging

Figure 23 was based on the Doppler ultrasonography of the femoral artery of the rat. The blood velocity in this vessel was 30.0 mm/s and no visual occlusion, stenosis, or thrombus was detected on the 30th day. Overall, the lumen diameter remained constant, signifying the total patency of the DEVG after tissue integration. The patency result was comparable to those of decellularized vascular graft [97, 127, 142–144] and synthetic vascular graft papers [145–150].

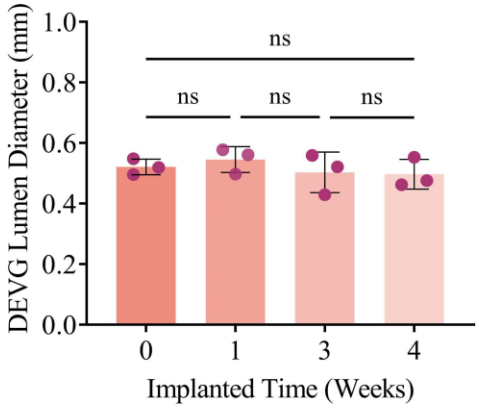

Figure 23. DEVG Lumen Diameter via Doppler Ultrasonography

Chapter 5 Conclusion and Future Directions

DEVG was designed as an implanted drug delivery system that could facilitate the targeted immunosuppression of T lymphocytes following organ transplantation. The inner layer consists of electrospun PLGA/PLCL nanofibers with interspersed tacrolimus. As the layer biodegrades, tacrolimus will be released from the matrix. Mechanical characterization of DEVG discovered the optimal composition of 50% PLCL and 50% PLGA, with the modulus of elasticity: 44.2 MPa (axial) and 9.3 MPa (circumferential), suture retention strength: 4.0 MPa, and pore diameter: 23.7 μm (day 0) and 13.9 μm (day 84). In vitro degradation of the PLGA/PLCL layer witnessed a 25.9% decrease in weight over 12 weeks, which corresponded to 60% of cumulative tacrolimus release from the DEVG. In vitro cytocompatibility assays reported the optimal tacrolimus loading concentration of 1 mg/graft. This concentration did not obstruct endothelial cell adhesion and angiogenesis, whilst still modulating the cytokine release of macrophages and activation cascade of T lymphocytes. The implantation of DEVG (length: 1–1.5 cm, diameter: 0.50 ± 0.02 mm, and loading concentration: 1.4–1.5 mg) into the femoral artery of a Sprague-Dawley rat was pronounced successful. The graft continually released tacrolimus at a concentration of 1.0–1.5 ng/ml/day and remained patent after 4 weeks of implantation.

Future research should scope the complexity of DEVG's in vivo performance. The experimental scheme should include subjects of negative control (sham subjects) and subjects of systemic drug administration (traditional approach) for therapeutic comparison. Additionally, the long-term effects of this biomaterial-mediated immunomodulation modality such as chronic inflammation, neuropathy, and neurotoxicity were not considered in this study, but they are crucial safety studies for the clinical implementation of an engineered vascular graft.

References

[1] Jouda, H.; Murillo, L.; Wang, T. Current Progress in Vascular Engineering and Its Clinical Applications. *Cells* **2022**, *11* (3), 493–493.

[2] Steucke, K. E.; Tracy, P. V.; Hald, E. S.; Hall, J. L.; Alford, P. W. Vascular Smooth Muscle Cell Functional Contractility Depends on Extracellular Mechanical Properties. *Journal of Biomechanics* **2015**, *48* (12), 3044–3051.

[3] Di, H.; Rätsep, M. T.; Chapman, A.; Boyd, R. Adventitial Fibroblasts in Vascular Structure and Function: The Role of Oxidative Stress and Beyond. *Canadian Journal of Physiology and Pharmacology* **2010**, *88* (3), 177–186.

[4] Bou-Gharios, G.; Ponticos, M.; Rajkumar, V.; Abraham, D. Extra-Cellular Matrix in Vascular Networks. *Cell Proliferation* **2004**, *37* (3), 207–220.

[5] Benrashid, E.; McCoy, C. C.; Youngwirth, L. M.; Kim, J.; Manson, R. J.; Otto, J. C.; Lawson, J. H. Tissue Engineered Vascular Grafts: Origins, Development, and Current Strategies for Clinical Application. *Methods* **2016**, *99*, 13–19.

[6] Ben-Shaul, S.; Landau, S.; Merdler, U.; Levenberg, S. Mature Vessel Networks in Engineered Tissue Promote Graft–Host Anastomosis and Prevent Graft Thrombosis. *Proceedings of the National Academy of Sciences of the United States of America* **2019**, *116* (8), 2955–2960.

[7] Pashneh-Tala, S.; MacNeil, S.; Claeyssens, F. The Tissue-Engineered Vascular Graft—Past, Present, and Future. *Tissue Engineering Part B-reviews* **2016**, *22* (1), 68–100.

[8] Radke, D.; Jia, W.; Sharma, D.; Fena, K.; Wang, G.; Goldman, J.; Zhao, F. Tissue Engineering at the Blood-Contacting Surface: A Review of Challenges and Strategies in Vascular Graft Development. *Advanced Healthcare Materials* **2018**, *7* (15), 1701461–1701461.

[9] Ravi, S.; Chaikof, E. L. Biomaterials for Vascular Tissue Engineering. *Regenerative Medicine* **2010**, *5* (1), 107–120.

[10] Langer, R.; Vacanti, J. P. Tissue Engineering. *Science* **1993**, *260* (5110), 920–926.

[11] Matsuzaki, Y.; Kelly, J.; Shoji, T.; Shinoka, T. The Evolution of Tissue Engineered Vascular Graft Technologies: From Preclinical Trials to Advancing Patient Care. *Applied Sciences* **2019**, *9* (7), 1274–1274.

[12] Nikolova, M. P.; Chavali, M. Recent Advances in Biomaterials for 3D Scaffolds: A Review. *Bioactive Materials* **2019**, *4* (1), 271–292.

[13] Calori, I.; Braga, G.; da Costa Carvalho de Jesus, P.; Hong, B.; Tedesco, A. Polymer Scaffolds as Drug Delivery Systems. *European Polymer Journal* **2020**, *129* (1), 109621.

[14] Zielińska, A.; Karczewski, J.; Eder, P.; Kolanowski, T.; Szalata, M.; Wielgus, K.; Szalata, M.; Kim, D.; Shin, S.; Słomski, R.; Souto, E. B. Scaffolds for Drug Delivery and Tissue Engineering: The Role of Genetics. *Journal of Controlled Release* **2023**, *359* (1), 207–223.

[15] Lumsden, A. B.; Morrissey, N. J.; Staffa, R.; Lindner, J.; Janoušek, L.; Třeška, V.; Štádler, P.; Moursi, M. M.; Storck, M.; Johansen, K.; Schermerhorn, M. L.; Powell, R. J.; Panneton, J. M.; Zhou, W.; Naoum, J. J.; Lipsitz, E. C.; Buckley, C. J.; Timaran, C. H.; Jordan, W. D.; Darling, R. Randomized Controlled Trial Comparing the Safety and Efficacy between the FUSION BIOLINE Heparin-Coated Vascular Graft and the Standard Expanded Polytetrafluoroethylene Graft for Femoropopliteal Bypass. *Journal of Vascular Surgery* **2015**, *61* (3), 703–712.

[16] Shemesh, D.; Goldin, I.; Hijazi, J.; Zaghal, I.; Berelowitz, D.; Verstandig, A.; Olsha, O. A Prospective Randomized Study of Heparin-Bonded Graft (Propaten) versus Standard Graft in Prosthetic Arteriovenous Access. *Journal of Vascular Surgery* **2015**, *62* (1), 115–122.

[17] Caracciolo, P. C.; Rial-Hermida, M. I.; Montini-Ballarin, F.; Abraham, G.; Concheiro, A. Surface-Modified Bioresorbable Electrospun Scaffolds for Improving Hemocompatibility of Vascular Grafts. *Materials Science and Engineering: C* **2017**, *75* (1), 1115–1127.

[18] Sung, H.; Meredith, C.; Johnson, C. B.; Galis, Z. S. The Effect of Scaffold Degradation Rate on Three-Dimensional Cell Growth and Angiogenesis. *Biomaterials* **2004**, *25* (26), 5735–5742.

[19] Kim, J. Y.; Chun, S. Y.; Lee, S. H.; Lih, E.; Kim, J.; Kim, D. H.; Ha, Y.; Chung, J.-W.; Lee, J. N.; Kim, B. S.; Kim, H. T.; Yoo, E. S.; Han, D. K.; Kwon, T. G.; Jang, B. I. In Vivo

Validation Model of a Novel Anti-Inflammatory Scaffold in Interleukin-10 Knockout Mouse. *Tissue Engineering and Regenerative Medicine* **2018**, *15* (4), 381–392.

[20] Leal, B. B. J.; Wakabayashi, N.; Oyama, K.; Kamiya, H.; Braghirolli, D.; Pranke, P. Vascular Tissue Engineering: Polymers and Methodologies for Small Caliber Vascular Grafts. *Frontiers in Cardiovascular Medicine* **2021**, *7* (1).

[21] Carrabba, M.; Madeddu, P. Current Strategies for the Manufacture of Small Size Tissue Engineering Vascular Grafts. *Frontiers in Bioengineering and Biotechnology* **2018**, *6* (1).

[22] Kannan, R. Y.; Salacinski, H. J.; Butler, P.; Hamilton, G.; Seifalian, A. M. Current Status of Prosthetic Bypass Grafts: A Review. *Journal of Biomedical Materials Research Part B* **2005**, *74B* (1), 570–581.

[23] Devillard, C. D.; Marquette, C. A. Vascular Tissue Engineering: Challenges and Requirements for an Ideal Large Scale Blood Vessel. *Frontiers in Bioengineering and Biotechnology* **2021**, *9* (1).

[24] Johnson, W. C.; Lee, K. K. A Comparative Evaluation of Polytetrafluoroethylene, Umbilical Vein, and Saphenous Vein Bypass Grafts for Femoral-Popliteal Above-Knee Revascularization: A Prospective Randomized Department of Veterans Affairs Cooperative Study. *Journal of Vascular Surgery* **2000**, *32* (2), 268–277.

[25] Li, X.; Greisler, H. P. Biomaterials in the Development and Future of Vascular Grafts. *Journal of Vascular Surgery* **2003**, *37* (2), 472–480.

[26] Chen, L.; He, H.; Wang, M.; Li, X.; Yin, H. Surface Coating of Polytetrafluoroethylene with Extracellular Matrix and Anti-CD34 Antibodies Facilitates Endothelialization and Inhibits Platelet Adhesion under Sheer Stress. *Tissue Engineering and Regenerative Medicine* **2017**, *14* (4), 359–370.

[27] Lee, K. S.; Kayumov, M.; Emechebe, G. A.; Kim, D. W.; Cho, H. J.; Jeong, Y.-J.; Lee, D.-W.; Park, J.-K.; Park, C. H.; Kim, C.-S.; Obiweluozor, F. O.; Jeong, I.-S. A Comparative Study of an Anti-Thrombotic Small-Diameter Vascular Graft with Commercially Available E-PTFE Graft

in a Porcine Carotid Model. *Tissue Engineering and Regenerative Medicine* **2022**, *19* (3), 537–551.

[28] Gabriel, M.; Niederer, K.; Becker, M. A.; Raynaud, C. M.; Vahl, C.; Frey, H. Tailoring Novel PTFE Surface Properties: Promoting Cell Adhesion and Antifouling Properties via a Wet Chemical Approach. *Bioconjugate Chemistry* **2016**, *27* (5), 1216–1221.

[29] Hamlin, G. W.; Rajah, S. M.; Crow, M. J.; Kester, R. C. Evaluation of the Thrombogenic Potential of Three Types of Arterial Graft Studied in an Artificial Circulation. *British Journal of Surgery* **1978**, *65* (4), 272–276.

[30] Allen, B. S.; Mathias, C. J.; Sicard, G. A.; Welch, M. J.; Clark, R. E. Platelet Deposition on Vascular Grafts. *Annals of Surgery* **1986**, *203* (3), 318–328.

[31] Kottke-Marchant, K.; Anderson, J. M.; Miller, K. M.; Marchant, R.; Lazarus, H. Vascular Graft-Associated Complement Activation and Leukocyte Adhesion in an Artificial Circulation. *Journal of Biomedical Materials Research* **1987**, *21* (3), 379–397.

[32] Rychlik, I. J.; Davey, P.; Murphy, J.; O'Donnell, M. E. A Meta-Analysis to Compare Dacron versus Polytetrafluroethylene Grafts for Above-Knee Femoropopliteal Artery Bypass. *Journal of Vascular Surgery* **2014**, *60* (2), 506–515.

[33] Seifalian, A. M.; Salacinski, H. J.; Tiwari, A.; Edwards, A. J.; Bowald, S.; Hamilton, G. In Vivo Biostability of a Poly(Carbonate-Urea)Urethane Graft. *Biomaterials* **2003**, *24* (14), 2549–2557.

[34] Wijeyaratne, S. M.; Kannangara, L. Safety and Efficacy of Electrospun Polycarbonate-Urethane Vascular Graft for Early Hemodialysis Access: First Clinical Results in Man. *The Journal of Vascular Access* **2016**, *12* (1).

[35] Eilenberg, M.; Enayati, M.; Ehebruster, D.; Grasl, C.; Walter, I.; Meßner, B.; Baudis, S.; Potzmann, P.; Kaun, C.; Podesser, B. K.; Wojta, J.; Bergmeister, H. Long Term Evaluation of Nanofibrous, Bioabsorbable Polycarbonate Urethane Grafts for Small Diameter Vessel Replacement in Rodents. *European Journal of Vascular and Endovascular Surgery* **2020**, *59* (4), 643–652.

[36] Hollister, S. J. Porous Scaffold Design for Tissue Engineering. *Nature Materials* **2005**, *4* (7), 518–524.

[37] Elomaa , L.; Yang, P. Additive Manufacturing of Vascular Grafts and Vascularized Tissue Constructs. *Tissue Engineering Part B: Reviews* **2017**, *23* (5).

[38] Ratner, B. D. Surface Modification of Polymers: Chemical, Biological, and Surface Analytical Challenges. *Biosensors and Bioelectronics* **1995**, *10* (9-10), 797–804.

[39] Middleton, J. C.; Tipton, A. T. Synthetic Biodegradable Polymers as Orthopedic Devices. *Biomaterials* **2000**, *21* (23), 2335–2346.

[40] Athanasiou, K. A.; Niederauer, G. G.; Agrawal, C. M. Sterilization, Toxicity, Biocompatibility and Clinical Applications of Polylactic Acid/ Polyglycolic Acid Copolymers. *Biomaterials* **1996**, *17* (2), 93–102.

[41] Donate, R.; Alemán-Domínguez, M. E.; Monzón, M. On the Effectiveness of Oxygen Plasma and Alkali Surface Treatments to Modify the Properties of Polylactic Acid Scaffolds. *Polymers* **2021**, *13* (10), 1643–1643.

[42] Zhang, Y.; Wang, J.; Xiao, J.; Fang, T.; Hu, N.; Li, M.; Deng, L.; Cheng, Y.-S.; Zhang, D.; Cui, W. An Electrospun Fiber-Covered Stent with Programmable Dual Drug Release for Endothelialization Acceleration and Lumen Stenosis Prevention. *Acta Biomaterialia* **2019**, *94* (1), 295–305.

[43] Dai, J.; Jin, J.; Yang, S.; Li, G. Doxorubicin-Loaded PLA/Pearl Electrospun Nanofibrous Scaffold for Drug Delivery and Tumor Cell Treatment. *Materials Research Express* **2017**, *4* (7), 075403–075403.

[44] Chen, J.; Zhang, D.; Wu, L.; Zhao, M. Current Strategies for Engineered Vascular Grafts and Vascularized Tissue Engineering. *Polymers* **2023**, *15* (9), 2015–2015.

[45] Tysoe, O.; Justin, A. W.; Brevini, T.; Chen, S. E.; Mahbubani, K. T.; Frank, A. K.; Zedira, H.; Melum, E.; Saeb-Parsy, K.; Markaki, A. E.; Vallier, L.; Sampaziotis, F. Isolation and

Propagation of Primary Human Cholangiocyte Organoids for the Generation of Bioengineered Biliary Tissue. *Nature Protocols* **2019**, *14* (6), 1884–1925.

[46] Hibino, N.; McGillicuddy, E. A.; Matsumura, G.; Ichihara, Y.; Naito, Y.; Breuer, C. K.; Shinoka, T. Late-Term Results of Tissue-Engineered Vascular Grafts in Humans. *The Journal of Thoracic and Cardiovascular Surgery* **2010**, *139* (2), 431–436.

[47] Zhang, G.; Zheng, G.; Ren, T.; Zeng, X.; Emile. Dopamine Hydrochloride and Carboxymethyl Chitosan Coatings for Multifilament Surgical Suture and Their Influence on Friction during Sliding Contact with Skin Substitute. *Friction* **2018**, *8* (1), 58–69.

[48] Melchiorri, A. J.; Hibino, N.; Brandes, Z. R.; Jonas, R. A.; Fisher, J. P. Development and Assessment of a Biodegradable Solvent Cast Polyester Fabric Small-Diameter Vascular Graft. *Journal of Biomedical Materials Research Part A* **2013**, *102* (6), 1972–1981.

[49] Fukunishi, T.; Best, C.; Sugiura, T.; Opfermann, J. D.; Ong, C. S.; Shinoka, T.; Breuer, C. K.; Krieger, A.; Johnson, J.; Hibino, N. Preclinical Study of Patient-Specific Cell-Free Nanofiber Tissue-Engineered Vascular Grafts Using 3-Dimensional Printing in a Sheep Model. *The Journal of Thoracic and Cardiovascular Surgery* **2017**, *153* (4), 924–932.

[50] Pektok, E.; Nottelet, B.; Tille, J.-C.; Gurny, R.; Kalangos, A.; Moeller, M.; Walpoth, B. H. Degradation and Healing Characteristics of Small-Diameter Poly(ε-Caprolactone) Vascular Grafts in the Rat Systemic Arterial Circulation. *Circulation* **2008**, *118* (24), 2563–2570.

[51] Woodward, S.; Brewer, P. S.; Moatamed, F.; Schindler, A.; Pitt, C. G. The Intracellular Degradation of Poly(ε-Caprolactone). *Journal of Biomedical Materials Research* **1985**, *19* (4), 437–444.

[52] Narayanan, G.; Shen, J.; Boy, R.; Gupta, B. S.; Tonelli, A. E. Aliphatic Polyester Nanofibers Functionalized with Cyclodextrins and Cyclodextrin-Guest Inclusion Complexes. *Polymers* **2018**, *10* (4), 428–428.

[53] Zhao, L.; Li, X.; Lei, Y.; Lu, H.; Mu, S.; Zong, H.; Li, Q.; Wang, F.; Song, S.; Yang, C.; Zhao, C.; Chen, H.; Zhang, R.; Wang, S.; Dong, Y.; Zhang, Q. Evaluation of Remodeling and

Regeneration of Electrospun PCL/Fibrin Vascular Grafts in Vivo. *Materials Science and Engineering: C* **2021**, *118* (1), 111441–111441.

[54] Jin, S.; Xue, X.; Huang, J. J.; Cheng, Y.; Zuo, Y.; Li, Y.; Li, J. Recent Advances in PLGA-Based Biomaterials for Bone Tissue Regeneration. *Acta Biomaterialia* **2021**, *127* (1), 56–79.

[55] Vu, T. P.; Conroy, J. P.; Yousefi, A. The Effect of Argon Plasma Surface Treatment on Poly(Lactic-Co-Glycolic Acid)/Collagen-Based Biomaterials for Bone Tissue Engineering. *Biomimetics* **2022**, *7* (4), 218–218.

[56] Yokota, T.; Ichikawa, H.; Matsumiya, G.; Kuratani, T.; Sakaguchi, T.; Iwai, S.; Shirakawa, Y.; Torikai, K.; Saito, A.; Uchimura, E.; Kawaguchi, N.; Matsuura, N.; Sawa, Y. In Situ Tissue Regeneration Using a Novel Tissue-Engineered, Small-Caliber Vascular Graft without Cell Seeding. *The Journal of Thoracic and Cardiovascular Surgery* **2008**, *136* (4), 900–907.

[57] Torikai, K.; Ichikawa, H.; Hirakawa, K.; Matsumiya, G.; Kuratani, T.; Iwai, S.; Saito, A.; Kawaguchi, N.; Matsuura, N.; Sawa, Y. A Self-Renewing, Tissue-Engineered Vascular Graft for Arterial Reconstruction. *The Journal of Thoracic and Cardiovascular Surgery* **2008**, *136* (1), 37-45.e1.

[58] Rocha, C. V.; Gonçalves, V.; da Silva, M. C.; Bañobre-López, M.; Gallo, J. PLGA-Based Composites for Various Biomedical Applications. *International Journal of Molecular Sciences* **2022**, *23* (4), 2034–2034.

[59] Laurent, C.; Vaquette, C.; Liu, X.; Schmitt, J.-F.; Rahouadj, R. Suitability of a PLCL Fibrous Scaffold for Soft Tissue Engineering Applications: A Combined Biological and Mechanical Characterisation. *Journal of Biomaterials Applications* **2018**, *32* (9), 1276–1288.

[60] Jang, B. S.; Cheon, J. Y.; Kim, J.; Park, W. H. Small Diameter Vascular Graft with Fibroblast Cells and Electrospun Poly (L-Lactide-*Co*-ε-Caprolactone) Scaffolds: Cell Matrix Engineering. *Journal of Biomaterials Science, Polymer Edition* **2017**, *29* (7-9), 942–959.

[61] Inoguchi, H.; Kwon, I. K.; Inoue, E.; Takamizawa, K.; Maehara, Y.; Matsuda, T. Mechanical Responses of a Compliant Electrospun Poly(L-Lactide-Co-ε-Caprolactone) Small-Diameter Vascular Graft. *Biomaterials* **2006**, *27* (8), 1470–1478.

[62] Horáková, J.; Mikeš, P.; Lukáš, D.; Saman, A.; Jenčová, V.; Klápšťová, A.; Svarcova, T.; Ackermann, M.; Novotný, V.; Kaláb, M.; Lonský, V.; Bartoš, M.; Rampichová, M.; Litvinec, A.; Kubíková, T.; Tomášek, P.; Tonar, Z. Electrospun Vascular Grafts Fabricated from Poly(L -Lactide-Co- E -Caprolactone) Used as a Bypass for the Rabbit Carotid Artery. *Biomedical Materials* **2018**, *13* (6).

[63] Huynh, T. T.; Abraham, G. A.; Murray, J.; Brockbank, K. G. M.; Hagen, P. O.; Sullivan, S. A. Remodeling of an Acellular Collagen Graft into a Physiologically Responsive Neovessel. *Nature Biotechnology* **1999**, *17* (11), 1083–1086.

[64] Devallière, J.; Chen, Y.; Dooley, K.; Yarmush, M. L.; Uygun, B. E. Improving Functional Re-Endothelialization of Acellular Liver Scaffold Using REDV Cell-Binding Domain. *Acta Biomaterialia* **2018**, *78* (1), 151–164.

[65] Liao, S.; He, Q.; Yang, L.; Liu, S.; Zhang, Z.; Guidoin, R.; Fu, Q.; Xie, X. Toward Endothelialization via Vascular Endothelial Growth Factor Immobilization on Cell-Repelling Functional Polyurethanes. *Journal of Biomedical Materials Research Part B* **2018**, *107* (4), 965–977.

[66] Copes, F.; Pien, N.; Vlierberghe, S. V.; Boccafoschi, F.; Mantovani, D. Collagen-Based Tissue Engineering Strategies for Vascular Medicine. *Frontiers in Bioengineering and Biotechnology* **2019**, *7* (1).

[67] Marcolin, C.; Draghi, L.; Tanzi, M. C.; Farè, S. Electrospun Silk Fibroin–Gelatin Composite Tubular Matrices as Scaffolds for Small Diameter Blood Vessel Regeneration. *Journal of Materials Science: Materials in Medicine* **2017**, *28* (5).

[68] Bertram, U.; Steiner, D.; Poppitz, B.; Dippold, D.; Köhn, K.; Beier, J. P.; Detsch, R.; Boccaccını, A. R.; Schubert, D. W.; Horch, R. E.; Arkudas, A. Vascular Tissue Engineering: Effects of Integrating Collagen into a PCL Based Nanofiber Material. *BioMed Research International* **2017**, *2017* (1), 1–11.

[69] Zhang, F.; Xie, Y.; Çelik, H.; Akkuş, O.; Bernacki, S. H.; King, M. W. Engineering Small-Caliber Vascular Grafts from Collagen Filaments and Nanofibers with Comparable Mechanical Properties to Native Vessels. *Biofabrication* **2019**, *11* (3), 035020–035020.

[70] Hu, Y.; Pan, X.; Zheng, J.; Ma, W.-G.; Sun, L. In Vitro and in Vivo Evaluation of a Small-Caliber Coaxial Electrospun Vascular Graft Loaded with Heparin and VEGF. *International Journal of Surgery* **2017**, *44* (1), 244–249.

[71] Nguyen, T.; Shojaee, M.; Bashur, C. A.; Kishore, V. Electrochemical Fabrication of a Biomimetic Elastin-Containing Bi-Layered Scaffold for Vascular Tissue Engineering. *Biofabrication* **2018**, *11* (1), 015007–015007.

[72] Li, D. Y.; Brooke, B. S.; Davis, E. C.; Mecham, R. P.; Sorensen, L. K.; Boak, B. B.; Eichwald, E. J.; Keating, M. T. Elastin Is an Essential Determinant of Arterial Morphogenesis. *Nature* **1998**, *393* (6682), 276–280.

[73] Ahsan, S. M.; Thomas, M.; Reddy, K. K.; Sooraparaju, S. S.; Asthana, A.; Bhatnagar, I. Chitosan as Biomaterial in Drug Delivery and Tissue Engineering. *International Journal of Biological Macromolecules* **2018**, *110* (1), 97–109.

[74] Yin, A.; Zhuang, W.; Liu, G.; Lan, X.; Tang, Z.; Deng, Y.; Wang, Y. Performance of PEGylated Chitosan and Poly (L-Lactic Acid-Co-ε-Caprolactone) Bilayer Vascular Grafts in a Canine Femoral Artery Model. *Colloids and Surfaces B: Biointerfaces* **2020**, *188* (1), 110806–110806.

[75] Fukunishi, T.; Best, C.; Sugiura, T.; Shoji, T.; Yi, T.; Udelsman, B. V.; Ohst, D. G.; Ong, C. S.; Zhang, H.; Toshiharu Shinoka; Breuer, C. K.; Johnson, J.; Hibino, N. Tissue-Engineered Small Diameter Arterial Vascular Grafts from Cell-Free Nanofiber PCL/Chitosan Scaffolds in a Sheep Model. *PLOS ONE* **2016**, *11* (7), e0158555–e0158555.

[76] Bochenek, M. A.; Veiseh, O.; Vegas, A. J.; McGarrigle, J. J.; Qi, M.; Marchese, E.; Omami, M.; Doloff, J. C.; Mendoza-Elias, J. E.; Nourmohammadzadeh, M.; Khan, A.; Yeh, C. C.; Xing, Y.; Isa, D.; Ghani, S.; Li, J.; Landry, C.; Báder, A.; Olejnik, K.; Chen, M. Alginate

Encapsulation as Long-Term Immune Protection of Allogeneic Pancreatic Islet Cells Transplanted into the Omental Bursa of Macaques. *Nature Biomedical Engineering* **2018**, *2* (11), 810–821.

[77] Antunes, M.; Bonani, W.; Reis, R. L.; Migliaresi, C.; Ferreira, H.; Motta, A.; Neves, N. M. Development of Alginate-Based Hydrogels for Blood Vessel Engineering. *Biomaterials Advances* **2022**, *134* (1), 112588–112588.

[78] Gaynor, J. J.; Ciancio, G.; Guerra, G.; Sageshima, J.; Hanson, L.; Roth, D.; Chen, L.; Kupin, W.; Mattiazzi, A.; Tueros, L.; Flores, S.; Aminsharifi, J.; Joshi, S.; Chediak, Z.; Ruiz, P.; Vianna, R.; Burke, G. W. Graft Failure due to Noncompliance among 628 Kidney Transplant Recipients with Long-Term Follow-Up. *Transplantation* **2014**, *97* (9), 925–933.

[79] Gordon, E. J.; Prohaska, T. R.; Gallant, M. P.; Siminoff, L. A. Adherence to Immunosuppression: A Prospective Diary Study. *Transplantation Proceedings* **2007**, *39* (10), 3081–3085.

[80] Zappasodi, R.; Budhu, S.; Abu-Akeel, M.; Merghoub, T. In Vitro Assays for Effector T Cell Functions and Activity of Immunomodulatory Antibodies. *Methods in Enzymology* **2020**, *631* (1), 43–59.

[81] Yılmaz, D.; Kirschner, K. M.; Demirci, H.; Himmerkus, N.; Bachmann, S.; Mutig, K. Immunosuppressive Calcineurin Inhibitor Cyclosporine Induces Proapoptotic Endoplasmic Reticulum Stress in Renal Tubular Cells. *Journal of Biological Chemistry* **2022**, *298* (3), 101589–101589.

[82] Schreiber, S. L.; Crabtree, G. R. The Mechanism of Action of Cyclosporin a and FK506. *Immunology Today* **1992**, *13* (4), 136–142.

[83] Mochizuki, M.; Masuda, K.; Sakane, T.; Itō, K.; Kogure, M.; Sugino, N.; Usui, M.; Mizushima, Y.; Ohno, S.; Inaba, G.; Yoshitaka Miyanaga; Hayasaka, S.; Kōtaro Ōizumi. A Clinical Trial of FK506 in Refractory Uveitis. *American Journal of Ophthalmology* **1993**, *115* (6), 763–769.

[84] Jegasothy, B. V.; Ackerman, C. D.; Todo, S.; Fung, J. J.; Abu-Elmagd, K.; Starzl, T. E. Tacrolimus (FK 506) - New Therapeutic Agent for Severe Recalcitrant Psoriasis. *Archives of Dermatology* **1992**, *128* (6), 781–785.

[85] Ponticelli, C.; Reggiani, F.; Moroni, G. Old and New Calcineurin Inhibitors in Lupus Nephritis. *Journal of Clinical Medicine* **2021**, *10* (21), 4832–4832.

[86] Banas, B.; Krämer, B. K.; Krüger, B.; Kamar, N.; Nasrullah Undre. Long-Term Kidney Transplant Outcomes: Role of Prolonged-Release Tacrolimus. *Transplantation Proceedings* **2020**, *52* (1), 102–110.

[87] Kojima, R.; Yoshida, T.; Tasaki, H.; Umejima, H.; Maeda, M.; Higashi, Y.; Watanabe, S.; Oku, N. Release Mechanisms of Tacrolimus-Loaded PLGA and PLA Microspheres and Immunosuppressive Effects of the Microspheres in a Rat Heart Transplantation Model. *International Journal of Pharmaceutics* **2015**, *492* (1-2), 20–27.

[88] Wu, J.; Zheng, Z.; Chong, Y.; Li, X.; Pu, L.; Tang, Q.; Liu, Y.; Wang, X.; Wang, F.; Liang, G. Immune Responsive Release of Tacrolimus to Overcome Organ Transplant Rejection. *Advanced Materials* **2018**, *30* (45).

[89] Nasiri, B.; Row, S.; Smith, R. J.; Swartz, D. D.; Andreadis, S. T. Cell-Free Vascular Grafts That Grow with the Host. *Advanced Functional Materials* **2020**, *30* (48).

[90] Kirkton, R. D.; Santiago-Maysonet, M.; Lawson, J. H.; Tente, W. E.; Dahl, S.; Niklason, L. E.; Prichard, H. L. Bioengineered Human Acellular Vessels Recellularize and Evolve into Living Blood Vessels after Human Implantation. *Science Translational Medicine* **2019**, *11* (485).

[91] Bahmani, B.; Uehara, M.; Jiang, L.; Ordikhani, F.; Banouni, N.; Ichimura, T.; Solhjou, Z.; Furtmüller, G. J.; Brandacher, G.; Álvarez, D.; Andrian, von; Uchimura, K.; Xu, Q.; Vohra, I.; Yilmam, O. A.; Haik, Y.; Azzi, J.; Kasinath, V.; Bromberg, J. S.; McGrath, M. M. Targeted Delivery of Immune Therapeutics to Lymph Nodes Prolongs Cardiac Allograft Survival. *Journal of Clinical Investigation* **2018**, *128* (11), 4770–4786.

[92] Syedain, Z. H.; Graham, M. L.; Dunn, T. B.; O'Brien, T. J.; Johnson, S. L.; Schumacher, R. J.; Tranquillo, R. T. A Completely Biological "Off-The-Shelf" Arteriovenous Graft That Recellularizes in Baboons. *Science Translational Medicine* **2017**, *9* (414).

[93] Henry, J.; Yu, J. Z.; Wang, A.-J.; Lee, R. J.; Fang, J.; Li, S. Engineering the Mechanical and Biological Properties of Nanofibrous Vascular Grafts for *in Situ* Vascular Tissue Engineering. *IOP Science* **2017**, *9* (3), 035007–035007.

[94] Fleischer, S.; Tavakol, D. N.; Vunjak-Novakovic, G. From Arteries to Capillaries: Approaches to Engineering Human Vasculature. *Advanced Functional Materials* **2020**, *30* (37), 1910811–1910811.

[95] Mallis, P.; Kostakis, A.; Stavropoulos-Giokas, C.; Michalopoulos, E. Future Perspectives in Small-Diameter Vascular Graft Engineering. *Bioengineering* **2020**, *7* (4), 160–160.

[96] Rickel, A. P.; Deng, X.; Engebretson, D.; Hong, Z. Electrospun Nanofiber Scaffold for Vascular Tissue Engineering. *Materials Science and Engineering: C* **2021**, *129* (1), 112373–112373.

[97] Yang, Y.; Lei, D.; Zou, H.; Huang, S.; Yang, Q.; Li, S.; Qing, F.; Ye, X.; You, Z.; Zhao, Q. Hybrid Electrospun Rapamycin-Loaded Small-Diameter Decellularized Vascular Grafts Effectively Inhibit Intimal Hyperplasia. *Acta Biomaterialia* **2019**, *97* (1), 321–332.

[98] Qiu, X.; Lee, B. L. P.; Ning, X.; Murthy, N.; Dong, N.; Li, S. End-Point Immobilization of Heparin on Plasma-Treated Surface of Electrospun Polycarbonate-Urethane Vascular Graft. *Acta Biomaterialia* **2017**, *51* (1), 138–147.

[99] Tille, J. C.; de Valence, S.; Mandracchia, D.; Nottelet, B.; Innocente, F.; Gurny, R.; Möller, M.; Walpoth, B. H. Histologic Assessment of Drug-Eluting Grafts Related to Implantation Site. *Journal of Developmental Biology* **2016**, *4* (1), 11–11.

[100] Punnakitikashem, P.; Truong, D. D.; Menon, J. U.; Nguyen, K. T.; Hong, Y. Electrospun Biodegradable Elastic Polyurethane Scaffolds with Dipyridamole Release for Small Diameter Vascular Grafts. *Acta Biomaterialia* **2014**, *10* (11), 4618–4628.

[101] Innocente, F.; Mandracchia, D.; Pektok, E.; Nottelet, B.; Tille, J.-C.; de Valence, S.; Faggian, G.; Mazzucco, A.; Kalangos, A.; Gurny, R.; Moeller, M.; Walpoth, B. H. Paclitaxel-Eluting Biodegradable Synthetic Vascular Prostheses. *Circulation* **2009**, *120* (11), 37–45.

[102] Ingulli, E. Mechanism of Cellular Rejection in Transplantation. *Pediatric Nephrology* **2010**, *25* (1), 61–74.

[103] Yau, J. W.; Teoh, H.; Verma, S. Endothelial Cell Control of Thrombosis. *BMC Cardiovascular Disorders* **2015**, *15* (1).

[104] Wang, X.; Chan, V.; Corridon, P. R. Acellular Tissue-Engineered Vascular Grafts from Polymers: Methods, Achievements, Characterization, and Challenges. *Polymers* **2022**, *14* (22), 4825–4825.

[105] Hu, J.; Sun, X.; Ma, H.; Xie, C.; Chen, Y. E.; Peter, X. Porous Nanofibrous PLLA Scaffolds for Vascular Tissue Engineering. *Biomaterials* **2010**, *31* (31), 7971–7977.

[106] Gao, J.; Chen, S.; Tang, D.; Li, J.; Shi, J.; Wang, S. Mechanical Properties and Degradability of Electrospun PCL/PLGA Blended Scaffolds as Vascular Grafts. *Transactions of Tianjin University* **2018**, *25* (2), 152–160.

[107] Patel, P.; Patel, H.; Panchal, S. S.; Mehta, T. Formulation Strategies for Drug Delivery of Tacrolimus: An Overview. *International Journal of Pharmaceutical Investigation* **2012**, *2* (4), 169–175.

[108] Tajdaran, K.; Shoichet, M. S.; Gordon, T.; Borschel, G. H. A Novel Polymeric Drug Delivery System for Localized and Sustained Release of Tacrolimus (FK506). *Biotechnology and Bioengineering* **2015**, *112* (9), 1948–1953.

[109] Pranke, P.; Weibel, D. E.; Braghirolli, D. I. Electrospun Scaffolds of Biodegradable Polyesters: Manufacturing and Biomedical Application. In *Biodegradable Polymers*; Fakirov, S., Ed.; Wiley: New York, NY, 2015; pp. 155–190. https://doi.org/10.1002/9783527656950.ch7.

[110] Duarte, M.; Siqueira, N. M.; Prabhakaram, M. P.; Ramakrishna, S. Electrospinning and Electrospray of Bio-Based and Natural Polymers for Biomaterials Development. *Materials Science and Engineering: C* **2018**, *92* (1), 969–982.

[111] Nguyen, D. N.; Clasen, C.; den Mooter, G. V. Pharmaceutical Applications of Electrospraying. *Journal of Pharmaceutical Sciences* **2016**, *105* (9), 2601–2620.

[112] Elliott, M. B.; Ginn, B.; Fukunishi, T.; Bedja, D.; Suresh, A.; Chen, T.; Inoue, T.; Dietz, H. C.; Santhanam, L.; Mao, H.; Hibino, N.; Gerecht, S. Regenerative and Durable Small-Diameter Graft as an Arterial Conduit. *Proceedings of the National Academy of Sciences of the United States of America* **2019**, *116* (26), 12710–12719.

[113] Nguyen, K. T.; Su, S.; Sheng, A.-L.; Wawro, D.; Schwade, N. D.; Brouse, C. F.; Greilich, P. E.; Tang, L.; Eberhart, R. C. In Vitro Hemocompatibility Studies of Drug-Loaded Poly-(L-Lactic Acid) Fibers. *Biomaterials* **2003**, *24* (28), 5191–5201.

[114] Thoms, S.; Ali, A. I.; Jonczyk, R.; Scheper, T.; Blume, C. Tacrolimus Inhibits Angiogenesis and Induces Disaggregation of Endothelial Cells in Spheroids – Toxicity Testing in a 3D Cell Culture Approach. *Toxicology in Vitro* **2018**, *53* (1), 10–19.

[115] Baatout, S.; Cheţa, N. Matrigel: A Useful Tool to Study Endothelial Differentiation. *Romanian Journal of Internal Medicine* **1996**, *34* (3-4), 263–269.

[116] Dellacherie, M. O.; Seo, B. R.; Mooney, D. J. Macroscale Biomaterials Strategies for Local Immunomodulation. *Nature Reviews Materials* **2019**, *4* (6), 379–397.

[117] Shi, C.; Pamer, E. G. Monocyte Recruitment during Infection and Inflammation. *Nature Reviews Immunology* **2011**, *11* (11), 762–774.

[118] Buckley, C. D.; Gilroy, D. W.; Serhan, C. N.; Stockinger, B.; Tak, P. P. The Resolution of Inflammation. *Nature Reviews Immunology* **2012**, *13* (1), 59–66.

[119] Duque, G. A.; Descoteaux, A. Macrophage Cytokines: Involvement in Immunity and Infectious Diseases. *Frontiers in Immunology* **2014**, *5* (1), 491.

[120] Beutler, B. A. The Role of Tumor Necrosis Factor in Health and Disease. *The Journal of Rheumatology* **2023**, *57* (1).

[121] Palmieri, E. M.; Gonzalez-Cotto, M.; Baseler, W. A.; Davies, L. C.; Ghesquière, B.; Maio, N.; Rice, C. M.; Rouault, T. A.; Cassel, T.; Higashi, R. M.; Lane, A. N.; Fan, T. W.-M. .; Wink, D. A.; McVicar, D. W. Nitric Oxide Orchestrates Metabolic Rewiring in M1 Macrophages by Targeting Aconitase 2 and Pyruvate Dehydrogenase. *Nature Communications* **2020**, *11* (1).

[122] Ben-Sasson, S. Z.; Hu-Li, J.; Quiel, J.; Cauchetaux, S.; Ratner, M.; Shapira, I.; Dinarello, C. A.; Paul, W. E. IL-1 Acts Directly on CD4 T Cells to Enhance Their Antigen-Driven Expansion and Differentiation. *Proceedings of the National Academy of Sciences of the United States of America* **2009**, *106* (17), 7119–7124.

[123] Chadban, S. J.; Tesch, G. H.; Foti, R.; Lan, H. Y.; Atkins, R. C.; Nikolic-Paterson, D. J. Interleukin-10 Differentially Modulates MHC Class II Expression by Mesangial Cells and Macrophages in Vitro and in Vivo. *Immunology* **1998**, *94* (1), 72–78.

[124] Ortega-Gómez, A.; Perretti, M.; Soehnlein, O. Resolution of Inflammation: An Integrated View. *EMBO Molecular Medicine* **2013**, *5* (5), 661–674.

[125] Laskin, B. L.; Jiao, J.; Baluarte, H. J.; Amaral, S.; Furth, S. L.; Akimova, T.; Hancock, W. W.; Levine, M. H.; Reese, P. P.; Beier, U. H. The Effects of Tacrolimus on T-Cell Proliferation Are Short-Lived: A Pilot Analysis of Immune Function Testing. *Transplantation Direct* **2017**, *3* (8), e199.

[126] Sharma, N.; Zhao, Q.; Ni, B.; Elder, P.; Puto, M.; Benson, D. M.; Rosko, A.; Chaudhry, M.; Devarakonda, S.; Bumma, N.; Khan, A.; Vasu, S.; Jaglowski, S.; William, B. M.; Mims, A. S.; Choe, H.; Larkin, K.; Brammer, J. E.; Wall, S.; Grieselhuber, N. R. Effect of Early Post-Transplantation Tacrolimus Concentration on the Risk of Acute Graft-Versus-Host Disease in Allogenic Stem Cell Transplantation. *Cancers* **2021**, *13* (4), 613–613.

[127] Qiu, X.; Lee, B. L. P.; Wong, S. Y.; Ding, X.; Xu, K.; Zhao, W.; Wang, D.; Sochol, R. D.; Dong, N.; Li, S. Cellular Remodeling of Fibrotic Conduit as Vascular Graft. *Biomaterials* **2021**, *268* (1), 120565–120565.

[128] Yu, J.; Wang, A.; Tang, Z.; Justin, J.; Lee, B. L. P.; Zhu, Y.; Yuan, F.; Huang, F.; Li, S. The Effect of Stromal Cell-Derived Factor-1α/Heparin Coating of Biodegradable Vascular Grafts on the Recruitment of Both Endothelial and Smooth Muscle Progenitor Cells for Accelerated Regeneration. *Biomaterials* **2012**, *33* (32), 8062–8074.

[129] Duan, R.; Wang, Y.; Zhang, Y.; Wang, Z.; Du, F.; Du, B.; Su, D.; Liu, L.; Li, X.; Zhang, Q. Blending with Poly(L-Lactic Acid) Improves the Printability of Poly(L-Lactide-*Co*-Caprolactone) and Enhances the Potential Application in Cartilage Tissue Engineering. *ACS Omega* **2021**, *6* (28), 18300–18313.

[130] Faturechi, R.; Hashemi, A.; Abolfathi, N.; Solouk, A. Mechanical Guidelines on the Properties of Human Healthy Arteries in the Design and Fabrication of Vascular Grafts: Experimental Tests and Quasi-Linear Viscoelastic Model. *Acta of Bioengineering and Biomechanics* **2019**, *21* (3).

[131] Xin, M.; Wang, X.; Jiang, Y.; Zhang, B.; Li, K.; Li, Q. Suture Retention Strength of P(LLA-CL) Tissue-Engineered Vascular Grafts. *RSC Advances* **2019**, *9* (37), 21258–21264.

[132] Joseph, J.; Bruno, V. D.; Sulaiman, N.; Ward, A. J.; Johnson, T.; Baby, H. M.; Varma, P. K.; Jose, R.; Nair, S. V.; Menon, D.; George, S. J.; Ascione, R. A Novel Small Diameter Nanotextile Arterial Graft Is Associated with Surgical Feasibility and Safety and Increased Transmural Endothelial Ingrowth in Pig. *Journal of Nanobiotechnology* **2022**, *20* (1).

[133] Makadia, H. K.; Siegel, S. J. Poly Lactic-Co-Glycolic Acid (PLGA) as Biodegradable Controlled Drug Delivery Carrier. *Polymers* **2011**, *3* (3), 1377–1397.

[134] Vaquette, C.; Cooper-White, J. J. Increasing Electrospun Scaffold Pore Size with Tailored Collectors for Improved Cell Penetration. *Acta Biomaterialia* **2011**, *7* (6), 2544–2557.

[135] Meyer, N.; Brodowski, L.; von Kaisenberg, C.; Schröder-Heurich, B.; von Versen-Höynck, F. Cyclosporine a and Tacrolimus Induce Functional Impairment and Inflammatory Reactions in Endothelial Progenitor Cells. *International Journal of Molecular Sciences* **2021**, *22* (18), 9696–9696.

[136] Eguchi, R.; Kubo, S.; Ohta, T.; Kunimasa, K.; Okada, M.; Tamaki, H.; Kaji, K.; Wakabayashi, I.; Fujimori, Y.; Ogawa, H. FK506 Induces Endothelial Dysfunction through Attenuation of Akt and ERK1/2 Independently of Calcineurin Inhibition and the Caspase Pathway. *Cellular Signalling* **2013**, *25* (9), 1731–1738.

[137] Sender, R.; Weiss, Y.; Navon, Y.; Milo, I.; Azulay, N.; Keren, L.; Fuchs, S.; Ben-Zvi, D.; Noor, E.; Milo, R. The Total Mass, Number, and Distribution of Immune Cells in the Human Body. *Proceedings of the National Academy of Sciences of the United States of America* **2023**, *120* (44).

[138] Yoshino, T.; Nakase, H.; Honzawa, Y.; Matsumura, K.; Yamamoto, S.; Takeda, Y.; Ueno, S.; Uza, N.; Masuda, S.; Inui, K. I.; Chiba, T. Immunosuppressive Effects of Tacrolimus on Macrophages Ameliorate Experimental Colitis. *Inflammatory Bowel Diseases* **2010**, *16* (12), 2022–2033.

[139] Kraaijeveld, R.; Li, Y.; Lin, Y.; de Leur, K.; Dieterich, M.; Peeters, A. M. A.; Wang, L.; Shi, Y.; Baan, C. C. Inhibition of T Helper Cell Differentiation by Tacrolimus or Sirolimus Results in Reduced B-Cell Activation: Effects on T Follicular Helper Cells. *Transplantation Proceedings* **2019**, *51* (10), 3463–3473.

[140] Alshamsan, A.; Binkhathlan, Z.; Kalam, M. A.; Qamar, W.; Kfouri, H.; Alghonaim, M.; Lavasanifar, A. Mitigation of Tacrolimus-Associated Nephrotoxicity by PLGA Nanoparticulate Delivery Following Multiple Dosing to Mice While Maintaining Its Immunosuppressive Activity. *Scientific Reports* **2020**, *10* (1).

[141] Dzhonova, D. V.; Olariu, R.; Leckenby, J. I.; Banz, Y.; Prost, J.-C.; Dhayani, A.; Vemula, P. K.; Voegelin, E.; Taddeo, A.; Rieben, R. Local Injections of Tacrolimus-Loaded Hydrogel Reduce Systemic Immunosuppression-Related Toxicity in Vascularized Composite Allotransplantation. *Transplantation* **2018**, *102* (10), 1684–1694.

[142] Kaushal, S.; Amiel, G. E.; Guleserian, K. J.; Shapira, O. M.; Perry, T. E.; Sutherland, F. W. H.; Rabkin, E.; Moran, A. M.; Schöen, F. J.; Atala, A.; Söker, S.; Bischoff, J.; Mayer, J. E. Functional Small-Diameter Neovessels Created Using Endothelial Progenitor Cells Expanded Ex Vivo. *Nature Medicine* **2001**, *7* (9), 1035–1040.

[143] Quint, C.; Kondo, Y.; Manson, R. J.; Lawson, J. H.; Dardik, A.; Niklason, L. E. Decellularized Tissue-Engineered Blood Vessel as an Arterial Conduit. *Proceedings of the National Academy of Sciences of the United States of America* **2011**, *108* (22), 9214–9219.

[144] Lee, S. H.; Lee, B. W.; Kim, S. W.; Choo, S. J. The Effects of Losartan in Preserving the Structural Integrity of Decellularized Small Diameter Vascular Allograft Conduit Implants in Vivo. *Artificial Organs* **2016**, *41* (1), 98–106.

[145] Prager, M.; Polterauer, P.; Böhmig, H. J.; Wagner, O.; Fügl, A.; Kretschmer, G.; Plohner, M.; Nanobashvili, J.; Huk, I. Collagen versus Gelatin-Coated Dacron versus Stretch Polytetrafluoroethylene in Abdominal Aortic Bifurcation Graft Surgery: Results of a Seven-Year Prospective, Randomized Multicenter Trial. *Surgery* **2001**, *130* (3), 408–414.

[146] Sevost'yanova, V. V.; Антонова, Л. В.; Великанова, Е. А.; Матвеева, В. Г.; Кривкина, Е. О.; Глушкова, Т. В.; Миронов, А. В.; Burago, A. Y.; Barbarash, L. S. Endothelialization of Polycaprolactone Vascular Graft under the Action of Locally Applied Vascular Endothelial Growth Factor. *Bulletin of Experimental Biology and Medicine* **2018**, *165* (2), 264–268.

[147] Guo, H.; Dai, W.; Qian, D.; Qin, Z.; Yan, L.; Hou, X.-Y.; Wen, C. A Simply Prepared Small-Diameter Artificial Blood Vessel That Promotes in Situ Endothelialization. *Acta Biomaterialia* **2017**, *54* (1), 107–116.

[148] Emechebe, G. A.; Obiweluozor, F. O.; Jeong, I. S.; Park, J.-K.; Park, C. H.; Kim, C. S. Merging 3D Printing with Electrospun Biodegradable Small-Caliber Vascular Grafts Immobilized with VEGF. *Nanomedicine: Nanotechnology, Biology and Medicine* **2020**, *30* (1), 102306–102306.

[149] Hou, J.; Zhang, X.; Wu, Y.; Jie, J.; Wang, Z.; Chen, G.; Sun, J.; Wu, L. Amphiphilic and Fatigue-Resistant Organohydrogels for Small-Diameter Vascular Grafts. *Science Advances* **2022**, *8* (30).

[150] Skovrind, I.; Harvald, E. B.; Belling, H. J.; Jorgensen, C.; Lindholt, J. S.; Andersen, D. C. Concise Review: Patency of Small-Diameter Tissue-Engineered Vascular Grafts: A Meta-Analysis of Preclinical Trials. *Stem Cells Translational Medicine* **2019**, *8* (7), 671–680.